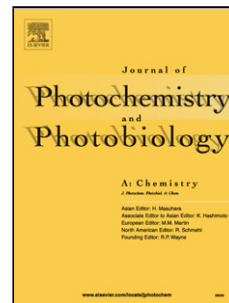


## Accepted Manuscript

Title: Pyrrole-thiazole based push-pull chromophores: An experimental and theoretical approach to structural, spectroscopic and NLO properties of the novel styryl dyes



Author: Kishor G. Thorat Nagaiyan Sekar

PII: S1010-6030(16)30399-9  
DOI: <http://dx.doi.org/doi:10.1016/j.jphotochem.2016.10.009>  
Reference: JPC 10393

To appear in: *Journal of Photochemistry and Photobiology A: Chemistry*

Received date: 24-5-2016  
Revised date: 3-10-2016  
Accepted date: 6-10-2016

Please cite this article as: {<http://dx.doi.org/>

This is a PDF file of an unedited manuscript that has been accepted for publication. As a service to our customers we are providing this early version of the manuscript. The manuscript will undergo copyediting, typesetting, and review of the resulting proof before it is published in its final form. Please note that during the production process errors may be discovered which could affect the content, and all legal disclaimers that apply to the journal pertain.

**Pyrrrole-Thiazole based Push-Pull Chromophores: An Experimental and Theoretical Approach to Structural, Spectroscopic and NLO Properties of the Novel Styryl Dyes**

Kishor G. Thorat and Nagaiyan Sekar\*

*Dyestuff Technology Department, Institute of Chemical Technology, Matunga,  
Mumbai-400 019, India.*

\*Corresponding author

Email: [n.sekar@ictmumbai.edu.in](mailto:n.sekar@ictmumbai.edu.in)/ [nethi.sekar@gmail.com](mailto:nethi.sekar@gmail.com)

Tel.: +91 22 3361 1111/ 2707; Fax: +91 22 3361 1020

---



- The said chromophores possess very high thermal decomposition temperatures ( $T_d$ ) which can make them suitable for use as potential NLO materials. Because of the high  $T_d$  the dyes can be safely incorporated into high temperature glass polymers and withstand high temperature fabrication steps of NLO devices.

**Abstract:** Novel push-pull fluorophores constituted by two donors (substituted pyrrole and morpholine) linked to acceptor through thiazole electron spacer have been synthesized. The fluorophores are investigated for linear and non-linear optical properties by UV-VIS absorption and fluorescence spectroscopies, and by means of TD-DFT (B3LYP/6-31G(d)) method, with the aim of elucidating the ability of the morpholine/pyrrole-donor-thiazole-spacer based D- $\pi$ -A fluorophores as organic NLO materials. The bond length alternation and generalized Mulliken-Hush (GMH) analysis is performed to understand the involvement of the donor in effective transfer of the charge to acceptor. Values of first-order hyperpolarizabilities ( $\beta_{CT}$  or  $\beta_0$ ), obtained by the solvatochromic method (Lippert Mataga model), and the transition dipole moments ( $\mu_{eg}$ ) used to characterize and evaluate the non-linear optical performances of the D- $\pi$ -A fluorophores in various microenvironments. The D- $\pi$ -A fluorophores possess good values of  $\beta_{CT}$  or  $\beta_0$  in different organic solvents and hold high thermal stabilities therefore can be used as potential organic NLO materials.

**Keywords:** Push-pull fluorophores, NLOs, Hyperpolarizability, CAM-B3LYP, BHLYP, BLA

---

## 1. Introduction

Electro optically active organic materials are currently being explored for their use in photonic devices, optical information handling and telecommunications[1–4]. Organic materials are known to have relatively strong non-linear optical properties owing to delocalized electrons at  $n \rightarrow \pi^*$  or  $\pi \rightarrow \pi^*$  orbitals[5–8]. This explains broad search for better NLO materials among organic molecules. In contrast to inorganic materials, the advent of dipolar conjugated organic materials with freely polarizable structures (hetero atoms at two extreme ends) was inspired by their relative comfort of synthesis, well-defined structure, chemical and thermal stabilities, possibility of additional modifications, and facile property tuning. Therefore, heteroaromatic push–pull chromophores have been examined as active constituents of organic light-emitting diodes (OLED), opto-electronic devices, semiconductors, switches, data-storage devices[9–11], etc.

Electro optic materials typically involve a host polymeric matrix comprising NLO chromophores either as guest molecules or covalently attached to the polymer support. Dipolar push-pull chromophores constitute the widespread class of compounds explored for their second harmonic generation (SHG) properties. These push-pull chromophores are mainly made of an electron donor (D) and an electron acceptor (A) group interacting through a  $\pi$ -conjugated spacer (Sp). It is well documented that the NLO activity of push-pull chromophores is determined not only by the strength of the D-A (Donor-Acceptor) pair, but also more subtly by the  $\pi$ -conjugated spacer[12–15].

It is well recognized that the first order hyperpolarizability ( $\beta_{xxx}$  or  $\beta_{CT}$ ), the combined magnitude ( $\beta_{CT\mu g}$ ) of molecular hyper susceptibilities, and the SHG (second harmonic

generation) values of microcrystal are normally used to describe the second-order NLO performance of organic compounds.

The most common method used to measure the  $\beta_{xxx}$  or  $\beta_{CT}$  values of organic compounds is an EFISHG (electronic field induced second harmonic generation) method, but this method is not easy to be set up for most laboratories[16,17]. The solvatochromic method used to measure first order hyperpolarizability ( $\beta_{xxx}$  or  $\beta_{CT}$ ) has been often preferred[18], because this study is easy to be built, although the values gained with the solvatochromic method are not as accurate as the values obtained with EFISHG method.

Recently, it was also recognized that push–pull systems applicable as organic materials should hold high chemical and thermal robustness, good solubility in various common organic solvents, and should be available in good quantities, therefore various five- and six-membered heterocycles were utilized as suitable  $\pi$ -conjugated chromophore backbones[15]. Also heteroatoms from the heterocyclic ring may act as auxiliary donors or acceptors and improve the total polarizability of the chromophore. Pyrroles, particularly ones substituted with alkyl groups at two or more positions, owing to their high reactivity towards electrophiles[19,20] are expected to show effective electron-hole charge transfer mechanism. Moreover, pyrroles can be easily prepared in good yields starting with simple, readily available organic materials[19] and can be further suitably functionalized at different positions[21]. Simple  $\pi$ -conjugated system such as olefins in push-pull chromophores can be replaced with spacer such as five or six membered heterocyclic compounds provide the rigidity to the conjugated system thus transpires effective intramolecular charge transfer and material expected to loose less energy non-radioactively as *cis-trans* isomerization is rendered. Also spacers such as, imidazole[15], thiophene[22], etc. are known to enhance the

thermal stability of the chromophore, which is crucial aspect as far as NLO chromophores are concerned. We thought the pyrrole donor in conjunction with thiazole spacer could help to enhance thermal as well as NLO properties of the push-pull chromophores.

With these perspectives, we have developed a series of push-pull chromophores constituted by two donors (D) (a substituted pyrrole and morpholine) and an acceptor (A) linked through a thiazole spacer (Sp) and investigated their structural and photophysical and hyperpolarizability properties in various microenvironments. Thermal stabilities of the chromophores were evaluated using DSC-TGA study which shows as expected very high thermal stabilities of the synthesized molecules. DFT and TD-DFT calculations were carried out at B3LYP/6-31G(d) level to get more insight on structural, photophysical, and NLO properties of these molecules. Generalized Milliken-Hush (GMH) and bond length alternation (BLA) analysis have been performed to estimate the charge transfer characteristics of the push-pull chromophores.

<<Please insert Figure 1 here>>

## 2. Experimental Section

### 2.1. General Methods

All the chemicals and spectroscopic grade solvents obtained from the local suppliers unless otherwise mentioned and used as such without further purifications and did not show any traces of fluorescence. All the common chemicals were of analytical grade. The solvents were purified by standard procedures. All the reactions were monitored by using TLC (thin-layer chromatography) with detection by UV light. The FT-IR spectra were recorded at room

temperature on a FT/IR Fourier Transform Infrared Spectrometer.  $^1\text{H}$  NMR,  $^{13}\text{C}$  NMR,  $^{11}\text{B}$  NMR and  $^{19}\text{F}$  NMR spectra were recorded on 500 MHz instrument using TMS as an internal standard. HRMS analysis was done using QTOF LC/MS, Mass spectra were recorded on the mass spectrometer. The thermal stability of the chromophores is determined by differential scanning calorimetry (DSC). The first order polarizability and first order hyperpolarizability were determined by using solvatochromic methods

## 2.2. *Photophysical studies*

The absorption spectra were recorded on the Perkin-Elmer UV/VIS spectrometer, Lambda 25. The emission spectra were recorded also at room temperature exciting at respective absorption maxima on VARIAN CARY Eclipse fluorescence spectrophotometer using 10 mm cuvette with 5 nm slit width. The excitation spectra were recorded using their respective emission maximum wavelengths on VARIAN CARY Eclipse fluorescence spectrophotometer using 10 mm cuvette with 5 nm slit width. The comparative fluorescence quantum yields ( $\phi_{\text{fl}}$ ) of the dyes **1-5** at their respective  $\lambda_{\text{abs}}$  maximum as excitation wavelength and 5 nm slit width determined using Nile red in ethanol ( $\phi_{\text{fl}}=0.12$ )[23] for dyes **1-4** and Nile blue-a perchlorate in ethanol ( $\phi_{\text{fl}}=0.27$ )[24] for the dye **5**.

## 2.3. *Computational details:*

The present calculations include the  $S_0$  state optimization of the dyes in vacuum and various solvent media followed by vertical excitation calculations and geometry optimization in the  $S_1$  state. Also vertical emission calculations have been performed. All the computations were performed using of the Gaussian 09 program package.[25] The geometries of the dyes in their  $S_0$  state were optimized using DFT[26] method.

The popular functional, B3LYP, (the B3LYP combines Becke's three parameter exchange functional (B3)[27] with the non-local correlation functional by Lee, Yang and Parr (LYP)[28] in conjunction with the basis set 6-31G(d) used in both, DFT and TD-DFT methods for all the atoms. Also frequency computations were performed at the same level of theory to verify whether the optimised structures have minimum energy. The vertical excitation energies and oscillator strengths were calculated for the first twenty  $S_0 \rightarrow S_1$  transitions at the optimized ground state ( $S_0$ ) equilibrium geometries by using TD-DFT with the same hybrid functional and basis set[29–36]. To obtain their minimum energy geometries (which correspond to the emissive state) the low-lying first singlet excited states ( $S_1$ ) of the dyes were relaxed using the TD-DFT. The emission wavelengths and oscillator strengths were obtained for the first ten  $S_1 \rightarrow S_0$  transitions at the optimized excited state equilibrium geometries by using the TD-DFT using the same hybrid functional and basis set[36,37]. All the computations in the different solvents media were carried out using the Self-Consistent Reaction Field (SCRF) using the CPCM polarizable conductor calculation model[38–40]. On the basis of the optimized ground structures, the electronic absorption and emission spectra, including maximum absorption and emission wavelengths, oscillator strengths, and main configuration assignment, were systematically investigated using TD-DFT with PCM model.

#### 2.4. Syntheses:

For the synthesis of the push-pull chromophores (dye **1-5**), we started with simple, inexpensive and readily available materials (Schemes 1 and 2). The compound **3** was synthesized from ethyl acetoacetate and acetyl acetone in good yields by using

reported protocol[41]. The compound **3** after bromination with Br<sub>2</sub> in CHCl<sub>3</sub> using catalytic amount of HBr at reflux temperature yielded compound **4** as a solid. Once the reaction is complete, as indicated by TLC, the excess solvent was evaporated and the obtained product was triturated and again dried under vacuum in order get rid of trapped bromine. Then the compound **4** was treated with morpholine-4-carbothioamide (**2**) in EtOH to compound **5**. Then the compound **5** was subjected to Vilsmeier Haack formylation to get corresponding carbaldehyde (**6**). The formylation at thiazole ring progresses even at room temperature (but at slower rate) as position next to sulfur is electron rich because it has got an electronic supply from both the donors (pyrrole and morpholine substituents). The compound **6** obtained was further subjected to Knoevenagel condensation with different active methylene/methyl groups to get desired push-pull chromophores, dye **1-4**/dye **5**, respectively.

<<Please insert Scheme 1 here>>

<<Please insert Scheme 2 here>>

On the other hand though there are many reports[42–45] for the synthesis of intermediate **1**, we developed relatively modified protocol for preparation of **1**. In short to the solution of ammonium thiocyanate in dry acetone was added benzoyl chloride and resulting mixture was heated to 55 °C, then to this was added solution of morpholine in dry acetone maintaining vigorous reflux. Further the compound **1** was converted to required intermediate, **2**, by following reported protocol[43].

#### 2.4.1. Synthesis of *N*-(morpholine-4-carbonothioyl) benzamide (**1**):

To the solution of ammonium thiocyanate (10 g, 0.13 moles) in dry acetone (250 mL) was added drop wise 15.3 mL (0.13 moles) of benzoyl chloride at 0 °C and

resulting mixture was heated to reflux with vigorous stirring for 15 min. Then heating was terminated and to this was added solution of 10.2 mL (0.13 moles) of morpholine in dry acetone (50 mL) over 5 min maintaining vigorous reflux. The reaction mixture was allowed to stir at reflux temperature for another 30 min and then poured on to the excess of ice-water mixture with vigorous stirring. The pale yellow solid formed was collected by filtration and liberally washed with cold water furnished the desired product in good yield (29.6 g, 91 %); Mp-153 °C (Literature Mp-153 °C-156 °C)[43].

#### 2.4.2. *Synthesis of Morpholine-4-carbothioamide (2):*

The solution of compound **1** (20 g, 0.08 moles) in 120 mL conc. HCl was stirred for 12 h at 75 °C using overhead stirrer. Then the reaction mixture was cooled to RT and to this was added few ice cubes. The resulting mixture was neutralized using liquid ammonia. The crude pale yellow solid obtained after filtration under vacuum was washed with ice cold water followed by dilute sodium bicarbonate solution furnished the desired product (**2**) as an off white solid. (9.3 g, 79.6%); Mp-175 to °C-176 °C (Literature Mp-176 °C to 177 °C)[43].

#### 2.4.3. *Synthesis of Ethyl 4-acetyl-3, 5-dimethyl-1H-pyrrole-2-carboxylate (3):*

The compound **3** was synthesized, following the reported protocol in the reference[41].

#### 2.4.4. *Synthesis of Ethyl 4-(2-bromoacetyl)-3, 5-dimethyl-1H-pyrrole-2-carboxylate (4):*

To the solution of **3** (3 g, 0.0144 moles) in 30 mL dry CHCl<sub>3</sub> was added 2 drops of HBr (48 % aq. solution) and the resulting mixture was heated to 60 °C for 5 min. Then

to this was added solution of Br<sub>2</sub> (2.29 g, 0.0278 moles) in dry CHCl<sub>3</sub> (15 mL) under N<sub>2</sub> atmosphere, maintaining the 55 °C -60 °C temperature. The reaction mixture was allowed to stir at 60 °C for 8 h. After completion of reaction, as indicated by TLC, the solvent was removed under vacuum and obtained dark solid was washed with saturated sodium bicarbonate followed by dilute aq. sodium sulphite and water, respectively. The obtained crude solid was recrystallized from 10 % ethyl acetate in n-hexane yielded the desired product in the form of white solid. Yield- 2.7 g (65.3 %); Mp- 128 °C; <sup>1</sup>H NMR (500 MHz, cdcl<sub>3</sub>) δ 9.40 (s, 1H), 4.35 (q, J = 7.1 Hz, 2H), 4.26 (s, 2H), 2.61 (s, 3H), 2.56 (s, 3H), 1.38 (t, J = 7.1 Hz, 3H); <sup>13</sup>C NMR (126 MHz, cdcl<sub>3</sub>) δ 188.2, 161.6, 139.6, 129.1, 120.5, 118.5, 60.6, 35.2, 15.1, 14.4, 12.5; MS (ESI) calcd for C<sub>11</sub>H<sub>15</sub>BrNO<sub>3</sub> (M+H)<sup>+</sup> 288.1 found 288.5.

*2.4.5. Synthesis of Ethyl 3,5-dimethyl-4-(2-morpholinthiazol-4-yl)-1H-pyrrole-2-carboxylate, (5):*

To the solution of **4** (2 g, 0.07 moles) in 30 mL absolute EtOH was added **2** (2.02 g, 0.0139 moles) and resulting mixture was allowed to stir at reflux temperature for 2 h. After completion of reaction, as indicated by TLC, the reaction mixture was allowed to cool to RT and to this was added cold water (70 mL). The off white solid precipitated out was collected by filtration under vacuum, washed three times with dilute aq. thiosulfate solution. The crude solid was purified by recrystallization using 25% ethyl acetate in n-hexane to get pale yellow solid in good yield (1.91 g, 82%). Mp- 148 °C; <sup>1</sup>H NMR (500 MHz, cdcl<sub>3</sub>) δ 8.73 (s, 1H), 6.36 (s, 1H), 4.31 (q, J = 7.1 Hz, 2H), 3.83 (t, J = 5 Hz, 4H), 3.49 (t, J = 5 Hz, 4H), 2.43 (s, 3H), 2.41 (s, 3H), 1.36 (t, J = 7.1 Hz, 3H); <sup>13</sup>C NMR (126 MHz, cdcl<sub>3</sub>) δ 170.5, 161.7, 146.7, 131.5, 118.6,

117.4, 103.0, 66.2, 59.8, 48.5, 14.5, 13.1, 11.8; HRMS (ESI)  $m/z$  calcd for  $C_{16}H_{22}N_3O_3S$  (M+H)<sup>+</sup> 336.1384; found 336.1352.

*2.4.6. Synthesis of Ethyl 4-(5-formyl-2-morpholinethiazol-4-yl)-3, 5-dimethyl-1H-pyrrole-2-carboxylate (6):*

POCl<sub>3</sub> (2.78 mL, 0.029 moles) was drop wise added at 0 °C to dry DMF (3.2 mL, 0.045 moles) under nitrogen atmosphere over 5 min. Then the mixture was allowed to warm to RT for 10 min. and again cooled to 0 °C, followed by drop wise addition of solution of compound **5** (5 g, 0.015 moles) in 10 mL dry DMF. The resulting reaction mixture was allowed to stir at 50 °C for 1 h. After completion of reaction, as indicated by TLC, the reaction mixture was cooled to RT and to this was added ice cold water (50 mL) and stirred for another 15-20 min. at RT. The pale yellow precipitate obtained was collected by filtration under vacuum, washed with saturated sodium bicarbonate solution followed by with water and dried. The obtained pale yellow solid (**6**) was used for next step without further purification. Yield= 4.85 g (89.6 %), Mp- 176 °C; <sup>1</sup>H NMR (500 MHz, cdcl<sub>3</sub>) δ 9.41 (s, 1H), 9.01 (s, 1H), 4.33 (q, J = 7.1 Hz, 2H), 3.83 (t, J = 5.5 Hz, 4H), 3.66 (t, J = 5.5 Hz, 4H), 2.33 (s, 3H), 2.31 (s, 3H), 1.36 (t, J = 7.1 Hz, 3H); <sup>13</sup>C NMR (126 MHz, cdcl<sub>3</sub>) δ 182.6, 173.7, 161.5, 159.3, 132.7, 127.9, 124.0, 118.6, 116.8, 66.0, 60.1, 48.2, 14.5, 12.5, 11.5; MS (ESI)  $m/z$  calcd for  $C_{17}H_{22}N_3O_4S$  (M+H)<sup>+</sup> 364.1333 found 364.1344.

*2.4.7. Synthesis of 2-(3-methylcyclohex-2-en-1-ylidene) malononitrile (7):*

The compound **7** was synthesized from 3, 5, 5-trimethylcyclohex-2-enone and malononitrile using the reported procedure[46]. Mp-77 °C -79 °C (Literature Mp-78 °C -80 °C)[47].

#### 2.4.8. General procedure for the synthesis of the dyes **1-5**:

To the solution of **6** (1 eq.) in absolute EtOH (15 mL) was added a drop of piperidine followed by addition of corresponding active methylene/ methyl compound (1.1 eq.). The resulting solution was allowed to stir under nitrogen atmosphere at reflux temperature for 12-24 h. After completion of reaction, as indicated by TLC, the reaction mixture was allowed to cool to room temperature and solid formed was collected by filtration under vacuum, washed with cold water. The crude solid obtained was purified by recrystallization from 80% EtOH (for the dyes **1-4**), the dye **5** was purified by column chromatography using 15 % ethyl acetate in toluene as eluent.

### 3. Results and Discussion

#### 3.1. Photophysical properties of the dyes **1-5**:

The experimental photophysical properties such as absorption maxima, emission maxima, full width at half absorption/ emission maximum (fwhm), Stokes shift, molar extinction coefficients, and quantum yield of fluorescence, etc. of the dyes, **1-5**, have been investigated in solvents of different polarities and results are collected in Table 1. The absorption and emission spectra of the dyes **1-5** in DMSO, are shown in Figure 2 and the absorption, excitation and emission spectra of the dyes **1-5** in various organic solvents is shown in Figures S1 to S10 (ESI), respectively (Please refer Figure 1 for molecular structures of the dyes **1-5**).

<<Please insert Figure 2 here>>

<<Please insert Table 1 here>>

The absorption spectra of the dyes **1-5** in DMSO shows one intense broad band with onset at around 375 to 400 nm and a maximum centered at around 447 nm, 453 nm, 453 nm, 478 nm and 535 nm, respectively. This major absorption band can be assigned to the combined ICT transition, from morpholine and pyrrole to the respective acceptor centre. The dyes **1** and **2** shows red shifted absorption with increase in solvent polarity that is from toluene ( $\lambda_{\text{abs}}$  is 432 nm and 440 nm, respectively) to DMSO ( $\lambda_{\text{abs}}$  is 447 nm and 453 nm, respectively). The dye **2** absorbs the radiations of slightly redder side (absorption maxima > by 5 -10 nm) compared to that of the dye **1** which can be attributed to the stronger electron pulling effect of second cyano group in the dye **2** compared to the carboxylate group in the dye **1**. Table 1 reveals that the dye **1** shows broader absorption band with larger  $\epsilon_{\text{max}}$  values compared to that of the dye **2**. The spectral properties of the dyes **3** and **4** can be compared with each other due to their structural and electronic similarities (Figure 1). The dye **4** compared to the dye **3** shows pronounced red shifted absorption (Table 1) in various organic solvents and this can be attributed to the sulphur atom present in the benzthiazole moiety, as it has got vacant d-orbitals which help to pull electron density from the donor (through the  $\pi$ -conjugated system) and effectively accommodate due to the presence of empty d-orbitals on it, overall lowering the gap between HOMO (highest occupied molecular orbital) and LUMO (lowest unoccupied molecular orbital). The dye **4** also shows red shift in absorption with increase in solvent polarity (Table 1). But absorption maxima of the dye **3** is influenced more in polar protic

solvents like EtOH and MeOH ( $\lambda_{\text{abs}}$  is 467 nm and 469 nm, respectively) compared to the polar aprotic solvents such as DMSO ( $\lambda_{\text{abs}}$  is 453 nm), DMF ( $\lambda_{\text{abs}}$  is 453 nm) and MeCN ( $\lambda_{\text{abs}}$  is 445 nm). This can be attributed to the hydrogen bonding arising between NH of benzimidazole of the dye **3** and protic solvent molecules in proximity causes restriction on rotation of benzimidazole fragment leading to the effective p-orbital overlap with donors (pyrrole and morpholine fragments) through spacer (thiazole) thus the dye **3** shows red shifted absorption in protic solvents compared to the less polar and polar aprotic solvents. The excitation spectra of the dyes **1-5** in various solvents are shown in Figures S1, S3, S5, S7 and S9 respectively (ESI) along with respective absorption spectra. From excitation spectra of the dyes **1-5** in various solvents it is seen that they shows similar profiles such as onset and maxima as that of corresponding absorption spectra thus the dyes can be excited over the range the respective excitation spectra covers.

The dye **5**, owing to its extra length of  $\pi$ -conjugation (Figure 1) between the donor-acceptor end points, possess highest values of absorption compared to the dyes **1-4** (Table 1). The absorption maxima of the dye **5** in different solvents are centered around 507 nm to 535 nm, with large fwhm, 101.6 nm to 123.6 nm from less polar to polar solvents, respectively. Also the dye **5**, possess the highest values of  $\epsilon_{\text{max}}$  in almost all the solvents studied, compared to that of the dyes **1-4** (Table 1).

The emission spectra were obtained using 5 nm slit width, and 10  $\mu\text{M}$  solute concentration, by exciting the samples at its wavelength of absorption maxima and results obtained are summarized in Table 1.

Table 1 and Figures S2 and S4 suggest that the dye **1** and **2** shows the broad emission bands relative to the corresponding absorption bands and are centered at around 488 nm to 499 nm and 491 nm to 505 nm in toluene to DMSO, respectively. In emission spectra positive solvatochromism is observed for both the dyes **1** and **2**. Compared to the dye **1**, the dye **2** shows emission at longer wavelengths (by 2-6 nm) in various solvents. The dyes **3** and **4** compared to corresponding absorption spectra shows a little broader emission bands with the maxima centered around 526 nm to 539 nm and 535 nm to 551 nm, respectively, in the solvents of different polarities.

Figures S9 and S10 and Table 1 reveal that the dye **5** compared to absorption shows sharper emission bands centered at 619 nm to 670 nm in different solvents. The emission maxima are highly influenced by solvent polarity with pronounced red shifts with an increase in solvent polarity. The dye **5** shows very large Stokes shifts, 112 nm in toluene to 158 nm in MeOH.

From Table 1 it can be seen that all the fluorophores under study (dyes **1-5**) possess poor quantum yields. The dyes **1** and **2** shows quantum yields of fluorescence ranging from 1.3 % in toluene to 9.4 % in chloroform for the dye **1** and 0.6 % in DMSO to 1.9 % in methanol for the dye **2**. The dyes **3** and **4** shows fluorescence quantum yields ( $\phi_f$ ) ranging from 1.7 % in DMSO to 3.6 % in DMF for the dye **3** and 0.2 % in ethyl acetate to 1.3 % in DMF for the dye **4**. The dye **5** possess good values of quantum yields of fluorescence ( $\phi_f$ ) ranging from 2.2 % in MeCN to 4.3 % in acetone. Reason for the observation of poor quantum yields is further discussed in section on TD-DFT calculated photophysical properties of the dyes **1-5**.

### 3.2. Solvatochromism:

Solvent dependent spectral properties of the chromophores, **1-5** were understood by the Lippert Mataga theory,[48–51]

$$\bar{\nu}_{abs} - \bar{\nu}_{ems} = \frac{2\Delta\mu_{CT}^2}{hc a^3} \left( \frac{\epsilon-1}{2\epsilon+1} - \frac{n^2-1}{2n-1} \right) + \text{Constant} \quad (1)$$

where,  $\bar{\nu}_{abs}$ , and  $\bar{\nu}_{ems}$  are wave numbers ( $\text{cm}^{-1}$ ) of absorption and emission maxima, respectively.  $h$  is Planck's constant ( $6.6256 \times 10^{-27}$  erg),  $c$  is the velocity of light ( $2.9979 \times 10^{10}$   $\text{cm s}^{-1}$ ),  $\Delta\mu_{CT}$  is the difference between the charge transfer excited ( $S_1$ ) state and ground ( $S_0$ ) state dipole moments.  $a$  is the cavity radius in which the molecule resides (in cm),  $\epsilon$  is relative dielectric constant and  $n$  is the refractive index of the solvent. The Onsager's radii ( $a$ ) for the dyes **1-5** in various solvents were calculated by integration of the solvent accessible surface using B3LYP/6-31G(d) ground state optimized geometry and summarized in Table 2.

<<Please insert Figure 3 here>>

The plots of variation of Stokes shift with the Lippert-Mataga polarity function for the dyes **1-5** are shown in Figure 3 (Plots A to E). From Figure 3 (plots A to E) it can be seen that there linear regressions with good values of factor of quality ( $R^2$ ) suggest the effective intramolecular charge transfer (ICT) between donor and acceptor end groups of the push-pull chromophores under investigation. From Figure 3 it can be seen that the Lippert Mataga plots A to D (the dyes **1-4**) shows negative slopes because there is increase in Stokes shift with decrease in solvent polarity (Table 1).

<<Please insert Table 2 here>>

The values of  $\Delta\mu_{CT}$  in different solvents were evaluated using Equation 3 and summarized in Table 2, which shows that among the dyes **1-5**, the dye **5** shows the highest change in dipole moments when excited from  $S_0$  to  $S_1$  state ( $3.46 \times 10^{-18}$  e.s.u to  $3.19 \times 10^{-18}$  e.s.u, in different solvents) followed by the dye **4**, then the dye **1** and the dye **2**. The dye **3** shows least values of the  $\Delta\mu_{CT}$  (Table 2). ICT characteristics of the dyes **1-5** are also studied with the help of generalized Mulliken-Hush (GMH) analysis and bond length alternation (BLA) studies.

### 3.3. Mulliken-Hush analysis of intramolecular charge transfer (ICT) states:

According to B. J. Coe et al. two state analysis of intramolecular charge transfer (ICT) gives,[52]

$$\Delta\mu_{ab}^2 = \Delta\mu_{ge}^2 + 4\mu_{ge}^2 \quad (2)$$

where,  $\Delta\mu_{ab}$  and  $\Delta\mu_{ge}$  are the dipole moment change between the diabatic states and the observed (adiabatic) dipole moment change, respectively.  $\mu_{ge}$  is the transition dipole moment.

The transition dipole moment ( $\mu_{ge}$ ) is related to the oscillator strength ( $f$ ) by following Equation 3,

$$\mu_{ge}^2 = \frac{3e^2h}{8\pi^2mc} X \frac{f}{\bar{\nu}_{eg}} \quad (3)$$

where,  $m$ ,  $f$ ,  $\bar{\nu}_{eg}$  and  $e$  are the mass of electron, oscillator strength, absorption frequency, and charge on electron respectively.  $h$  and  $c$  same as above.

The oscillator strength ( $f$ ), can be evaluated from integrated area of absorption coefficient ( $\int \epsilon(\nu) d\nu$ ) and refractive index of the medium ( $n$ ) by using the following Equation 4,

$$f = \frac{4.32 \times 10^{-9}}{n} \int \varepsilon(\vartheta) d\vartheta \quad (4)$$

Thus, by using the values of  $f$ , the values of  $\mu_{ge}$  for the dyes **1-5** in solvents of different polarity parameters are determined from Equation 3. The values of  $\mu_{ge}$  and  $f$  are summarized in Table 2. The values of oscillator strengths ( $f$ ) and transition dipole moments ( $\mu_{eg}$ ) for the dyes **1-5** were obtained using corresponding equations and summarized in Table 2. Table 2 reveals that, the dye **5** in different solvents shows the highest values of oscillator strengths (with minimum of 0.4663 e.s.u in toluene and maximum of 0.8956 e.s.u in MeOH) compared to the dyes **1-4**. The dyes **1** and **4** also shows good values of oscillator strength (0.4585 e.s.u and 0.5283 e.s.u in CHCl<sub>3</sub>, for the dyes **1** and **4**, respectively).

The dye **5**, among the dyes studied, possess highest values of transition dipole moments ( $\mu_{ge}$ ) with maximum of  $9.77 \times 10^{-18}$  e.s.u in MeOH and minimum of  $7.09 \times 10^{-18}$  e.s.u in toluene. The order of  $\mu_{ge}$  values among the dyes **1-5** is, dye **5** > dye **4** > dye **1** > dye **2** > dye **3** (Table 2). From Table 2 it can be seen that all the dyes under investigation possess good values of  $\mu_{ge}$  and  $f$  in solvents of various polarities suggesting an effective charge transfer from donor to the acceptor end group (Table 2). The degree of delocalization or fractional degree of localization of the excess charge ( $C_b^2$ ) and electronic coupling matrix ( $H_{DA}$ ) for the diabatic states are expressed by following Equations 5 and 6, respectively[53].

$$C_b^2 = \frac{1}{2} \left( 1 - \sqrt{\frac{\Delta\mu_{ge}^2}{\Delta\mu_{ge}^2 + 4\mu_{ge}^2}} \right) \quad (5)$$

$$H_{DA} = \frac{\Delta E_{ge} \mu_{ge}}{\Delta\mu_{ab}} \quad (6)$$

Electron coupling elements of electron transfer in D- $\pi$ -A is one of the key parameters that defines the rate of charge transfer over the compound which can be evaluated by using generalized Mulliken-Hush (GMH) fragment charge methods[54–56].

An competent charge transfer in D- $\pi$ -A system leading to charge transfer excited state in a D- $\pi$ -A chromophore is known to display of NLO properties.[57,58] Within two level approximation, the extent of donor-acceptor electronic coupling ( $H_{DA}$ ) between the  $S_0$  and charge transfer excited states is correlated with the vertical excitation energy ( $\Delta E_{ge}$ ), the difference between the adiabatic dipole moments of the ground and excited states ( $\Delta\mu_{ge}$ ), and the difference in diabatic state dipole moments and the transition dipole moments ( $\Delta\mu_{ge}^D$ ) by the generalized Mulliken-Hush (GMH) model[54,55,59] is expressed as Equation 7,

$$H_{DA} = \frac{\Delta E_{ge} \mu_{ge}}{\Delta\mu_{ge}^D} = \frac{\mu_{ge} \Delta E_{ge}}{\sqrt{\Delta\mu_{ge}^2 + 4 \mu_{ge}^2}} \quad (7)$$

The adiabatic states are assumed to be composed of these three diabatic states- a donor group state (GS), a donor locally excited state (LE), and a charge transfer state (CT) with transferring electron localized on the acceptor. This approach has been carefully used in a few charge transfer systems[56–58].

The extent of charge separation due to influence of donor-acceptor interactions through  $\pi$ -bridge can be evaluated from the following expression, Equation 8[59,60],

$$R_{DA} = 2.06 \times 10^{-2} \frac{\sqrt{\Delta E_{ge} \epsilon_{max} \Delta v_{1/2}}}{H_{DA}} \quad (8)$$

where,  $R_{DA}$  is separation between the centroids of the donor-acceptor orbitals ( $\text{\AA}$ ),  $\Delta E_{ge}$  is same as above ( $\text{cm}^{-1}$ ),  $\varepsilon_{max}$  is molar absorptivity ( $\text{M}^{-1} \text{cm}^{-1}$ ),  $\Delta\nu_{1/2}$  is bandwidth ( $\text{cm}^{-1}$ )  $H_{DA}$  is donor acceptor electronic coupling matrix or integral ( $\text{cm}^{-1}$ ).

The values of  $C_b^2$ ,  $H_{DA}$  and  $R_{DA}$  were estimated from Equations 5, 7 and 8, respectively, and summarized in Table 2. When  $C_b^2$  is zero then it is called total delocalization and when it is unity then it is called total localization of the charge[53]. From the values of the  $C_b^2$  (Table 2) it is seen that the dyes **1-5** possess good values of degree of delocalization in different microenvironments and thus the effective ICT characteristics.

As seen from the Equation 8,  $H_{DA}$  tend vary inversely with  $R_{DA}$  and vice versa. Thus the more the charge separation less is the extent of electronic coupling integral. Therefore among the dyes **1-5**, the dye **5** possess the lowest values of the  $H_{DA}$  as it has got the highest values of  $R_{DA}$  (Table 2).

### 3.4. NLO Properties-Solvatochromism and theoretical approach:

#### 3.4.1. NLO's of the push pull dyes, **1-5** using solvatochromic method:

The method used to determine the first ( $\alpha_{CT}$ ) and second ( $\beta_{xxx}$  or  $\beta_{CT}$ ) order polarizabilities of the push-pull chromophores, **1-5**, is based on solvatochromism[61,62].

##### 3.4.1.1. Determination of first polarizability ( $\alpha_{xx}$ or $\alpha_{CT}$ ) using solvatochromic method:

The usual NLO chromophores have an electron-donor group and an acceptor group connected through a  $\pi$ -conjugated system or spacer. Therefore, the  $S_1$  state is

frequently a low-lying charge-transfer state, typically in the visible or near-UV region of the electromagnetic spectrum. Hence, the dominant component of the first-order polarizability often referred as  $\alpha_{CT}$  whose apparent expression is [63,64],

$$\alpha_{CT} = 2 \frac{\mu_{eg}^2}{E_{eg}} = 2 \frac{\mu_{eg}^2 \lambda_{eg}}{E_{eg} hc} \quad (9)$$

where,  $x$ ,  $h$ ,  $c$ ,  $\lambda_{eg}$ ,  $E_{eg}$ ,  $\mu_{eg}$  are the direction of charge transfer, Planck's constant, velocity of light in vacuum, wavelength of transition from the  $S_0$  state to  $S_1$  state,  $S_0$  to  $S_1$  state transition energy and transition dipole moment, respectively. Using the values of  $\mu_{eg}$  in Equation 9, the values  $\alpha_{CT}$  for the dyes **1-5** in solvents of different polarities are calculated and summarized in Table 3.

<<Please insert Table 3 here>>

Table 3 reveals that the dye **5** compared to the dyes **1-4** possess the highest values of  $\alpha_{CT}$ , with minimum in  $\text{CHCl}_3$  ( $4.06 \times 10^{-23}$  e.s.u) and maximum in MeOH ( $4.81 \times 10^{-23}$  e.s.u). The values of the  $\alpha_{CT}$  for the dye **4** follows that of the dye **5** and also possess good values of  $\alpha_{CT}$  (Table 3) in different solvents studied.

#### 3.4.1.2. Determination of first order hyperpolarizability ( $\beta_{CT}$ ) using solvatochromic method:

The solvent dependent first order hyperpolarizability ( $\beta_{CT}$ ) is determined using two level microscopic model based on the Oudar Equation [65,66]. The modified form of Oudar Equation can be presented as,

$$\beta_{CT} = \frac{3v_{eg}^2 \mu_{eg}^2 \Delta\mu_{CT}}{2h^2 c^2 (v_{eg}^2 - v_L^2)(v_{eg}^2 - 4v_L^2)} \quad (10)$$

where,  $\vartheta_L$  is the frequency of the reference incident radiation to which the  $\beta_{CT}$  value would be referred.  $\vartheta_{eg}$  is the frequency and  $\Delta\mu_{CT}$  is same as above (Equation 1).

The values of  $\Delta\mu_{CT}$  and  $\mu_{eg}$  used in Equation 10 to evaluate the values of  $\beta_{CT}$  for the dyes **1-5** in different solvents, assuming  $\vartheta_L = 0$  *i. e.* assuming no excitation.

The two level microscopic model gives the rough estimation of the values of  $\beta_{CT}$  as the method is based on several assumptions and thus allow only rough estimate of leading tensor of total hyperpolarizability along the direction of charge transfer which is the major contributor to the  $\beta_{CT}$ . The values obtained for  $\beta_{CT}$  are summarized in Table 3. Table 3 reveals that the dyes **1-5** possess good values of the  $\beta_{CT}$ , of the order of  $10^{-30}$  e.s.u for the dyes **1-4** and that of  $10^{-29}$  e.s.u for the dye **5**. Among the dyes under study, the dye **5** shows highest values of  $\beta_{CT}$  (maximum of  $26.1 \times 10^{-30}$  e.s.u in MeOH and DMSO and minimum of  $13.62 \times 10^{-30}$  e.s.u in toluene) followed by the dye **4** (maximum of  $8.72 \times 10^{-30}$  e.s.u in  $\text{CHCl}_3$  and minimum of  $5.26 \times 10^{-30}$  e.s.u in toluene). Values of  $\beta_{CT}$  for the dye **1** (maximum of  $6.2 \times 10^{-30}$  e.s.u in acetone and minimum of  $4.42 \times 10^{-30}$  e.s.u in toluene) follows that of the dye **4**. The dyes **2** and **3** also shows good values of the  $\beta_{CT}$  (maximum of  $5.68 \times 10^{-30}$  e.s.u and  $5.72 \times 10^{-30}$  e.s.u in DMSO and minimum of  $1.85 \times 10^{-30}$  e.s.u and  $3.96 \times 10^{-30}$  e.s.u in toluene, for the dyes **2** and **3**, respectively). Thus the dyes **1-5** follows the order of NLO performances in DMSO solvent as dye **5** > dye **4** > dye **1** > dye **3** > dye **2**.

#### 3.4.2. NLO's of the dyes **1-5**, using TD-DFT (B3LYP/6-31G(d) method:

The static first hyperpolarizability ( $\beta_0$ ) and its related properties such as total static dipole moment ( $\mu$ ) and the mean polarizability ( $\alpha_0$ ) for dyes, **1-5** have been calculated using B3LYP functional with 6-31G(d) set on the basis of the finite-field

approach[67]. The Equations for calculating the magnitude of  $\mu$ ,  $\alpha_0$  and  $\beta_0$  using the  $x$ ,  $y$ ,  $z$  components from Gaussian 09 output are defined as follows[68],

The total static dipole moment ( $\mu$ ) is expressed by Equation 11,

$$\mu = \sqrt{\mu_x^2 + \mu_y^2 + \mu_z^2} \quad (11)$$

The isotropic polarizability ( $\alpha_0$ ) can be calculated from the trace of the polarization tensor using Equation 12,

$$\alpha_0 = \frac{(\alpha_{xx} + \alpha_{yy} + \alpha_{zz})}{3} \quad (12)$$

Equation 13 expresses the mean first order hyperpolarizability ( $\beta_0$ ),

$$\beta_0 = \sqrt{\beta_x^2 + \beta_y^2 + \beta_z^2} \quad (13)$$

The values calculated for  $\mu$ ,  $\alpha_0$  and  $\beta_0$  for the dyes **1-5**, in different solvents using Equations 11-13, respectively, are enlisted in Table 3.

From Table 3 it can be seen that the values of total static dipole moments for the dyes **1-5** increases with increase in the solvent polarity (from toluene to DMSO). Among the dyes under study, the dye **5** possess the highest values of total static dipole moments (from  $11.5 \times 10^{-17}$  e.s.u in toluene to  $15.1 \times 10^{-17}$  e.s.u in DMSO) followed by dye **2**, dye **4**, dye **1** and dye **3**, respectively (Table 3).

The values of the first polarizability ( $\alpha_0$ ) obtained with B3LYP/6-31G(d) method for the dyes **1-5** are very close to that obtained by solvatochromic method and moreover TD-DFT also suggest the maximum values for the dye **5** followed by the dye **4** (Table 3).

Different density functional theory methods such B3LYP/6-31G(d), CAM-B3LYP/6-31G(d) and BHHLYP/6-31G(d) employed to estimate the values of the first hyperpolarizability ( $\beta_0$ ) and values are summarized in Table 3. The values of the first hyperpolarizability ( $\beta_0$ ) produced with all the three methods are close to that obtained with solvatochromic methods and also follow same trend of the values of the  $\beta_0$  among the dyes **1-5** (Table 3). Out of the three methods the values of  $\beta_0$  obtained with CAM-B3LYP/6-31G(d) are slightly higher whereas that obtained with BHHLYP/6-31G(d) are slightly lower compared to that estimated by B3LYP/6-31G(d) method.

### 3.5. *Thermal Stability Properties:*

The thermal stabilities of the dyes **1-5** were determined by DSC–TGA studies and respective TGA curves are presented in Figure 4 and thermal decomposition temperatures ( $T_d$ ) at 10 % weight loss are in Table S1 (ESI). The samples were heated in a pan at a rate of 20 °C/min to give the onset of the  $T_d$ .

<<Please insert Figure 4 here>>

The  $T_d$  are defined as shown in Figure 4, being 346.7 °C for the dye **1**, 322.6 °C for the dye **2**, 337.8 °C for the dye **3**, 351.4 °C for the dye **4** and 374.3 °C for the dye **5**, reveal the order of thermal stability for the dyes **1-5** is dye **5** > dye **4** > dye **1** > dye **3** > dye **2**.

Thus, the NLO chromophores, dyes **1-5**, found to be thermally very stable and shows  $T_d$  between 322.6 °C and 374.3 °C, which proves them to be a good chromophores for the incorporation into high temperature glass ( $T_g$ ) polymers (such as polyetherketone, polyimide, etc.).

It is pointed out that the TGA result of the dyes **2** and **3** reveals two stages of weight reduction. The first stage beginning at about 100 °C may be caused by the evaporation of traces of water/moisture present and the onset of the second stage was defined as the  $T_d$  of the dyes **2** and **3**. The dye **5** shows three stages of weight reduction, one at around 100 °C can be attributed to the evaporation of moisture content, second at 245 °C may be because of sublimation of the compound and the last one at 374.3 °C is corresponds to its  $T_d$ .

Thus, the dyes (**1-5**) possess considerably higher thermal stabilities compared to that of the commercially available NLO push-pull chromophores, such as DR1 ( $T_d=254$  °C),[69] DO3 ( $T_d=235$  °C) and DR19 ( $T_d=260$  °C)[70], and also the dyes **1-5** are thermally more stable than the recently reported NLO chromophores[71], such as TPA-H ( $T_d=298.4$  °C) and TPA-CN ( $T_d=300.7$  °C) which demonstrates them more suitable for use as semi-conductor laser materials[62] and thermally robust at high temperatures to withstand fabrication steps for those devices.

### 3.6. *Theoretical studies:*

The density functional theory (DFT)[26] and time dependent density functional theory (TD-DFT)[26] with B3LYP/6-31G(d)[26–28] level were employed to gain more understanding of the electronic, structural, photophysical and hyperpolarizability properties of push-pull chromophores under study. The unconstrained geometries of the compounds in their  $S_0$  and  $S_1$  states in vacuum as well as various microenvironments were optimized by DFT using the Becke's three-parameter functional[27] hybridized with the Lee–Yang–Parr correlation functional[28] and the 6-31G(d,) basis set[29–36,72,73].

*3.6.1. Ground ( $S_0$ ) and the lowest-lying singlet ( $S_1$ ) excited state geometries of the push-pull chromophores (dyes 1-5):*

The main TD-DFT optimized geometrical parameters of the styryl derivatives (dyes **1-5**) in its  $S_0$  and  $S_1$  states are shown in Figures 5 to 7 and summarized in the Table S2 (ESI). The dyes **1-5**, in their optimized  $S_0$  state having geometry with the morpholine donor, thiazole spacer and corresponding acceptor end groups a perfectly planar arrangements with pyrrole moiety twisted by about  $49^\circ$ - $54^\circ$  (Figures 5-7 and Table S2). The twisting between pyrrole and thiazole moieties in the  $S_1$  state of the dyes **1-5** is decreased by few degrees ( $3^\circ$  to  $8^\circ$ , Figures 5-7 and Table S2) increasing  $p$ -orbitals overlap between donor pyrrole and spacer thiazole groups.

<<Please insert Figure 5 here>>

<<Please insert Figure 6 here>>

<<Please insert Figure 7 here>>

Figures 5 to 7 and Table S2 reveal that the lengths of the bond between donor-acceptor end groups are altered, that is the lengths of the double bonds are increased and that of single bonds are decreased when excited from  $S_0$  to  $S_1$  state. The bond length between N1-C1 and that of N1'-C1' is decreased and bond length between C6-N3 (dyes **1-4**) and C10-N3 (dye **5**) increased in the excited ( $S_1$ ) state, signifies the direction of the flow of electrons, thus the charge transfer from donors to acceptor end groups through spacer thiazole. The decrease in the dihedral angle between donor pyrrole and spacer thiazole in  $S_1$  state of the dyes **1-5** and also alteration of bond lengths (N1'-C1', C1'-C2' and C2'-C2) clearly indicates the involvement of the

pyrrole ring in the intramolecular charge transfer assisted by twisting, from pyrrole donor to the corresponding acceptor end group. The values of dihedral angles (C3-C4-C5-C6) for all the dyes under study suggests the corresponding acceptor end groups make an perfectly planar arrangements with the spacer and morpholine donor end group allowing effective  $p$ -orbitals overlap. Thus, an effective intramolecular charge transfer prevails between the donor and acceptor end groups. Conversely, there is little increase in C3-C4-C5-C6 torsional angle in the dyes **1-5** when excited to  $S_1$  and this may be the reason for enlargement of the C4-C5 bond length in the  $S_1$  state of the dyes **1-5** (Table S2). Lippert- Mataga solvent polarity function also support the ICT characteristics of the dyes. Hence the ICT characteristics of the dyes were taken in to account for evaluation of the NLO properties of the dyes under investigation. The benzimidazole and benzthiazole moieties in the dyes **3** and **4** also possess perfectly planar arrangements (Figure 6) and hence owing to the increased length of  $\pi$ -conjugation shows red shifted absorption and emission maxima compared to the dyes **1** and **2** (Table 1). The dye **5** has got extra length of  $\pi$ -conjugation (Figure 7) compared to the dyes **1-4** (Figures 5 and 6) leading to decreased HOMO-LUMO band gap, thus shows the highest values of absorption and emission.

### 3.6.2. Bond length alternation (BLA):

The bond length alternation (BLA) is a geometrical parameter and calculated as the difference between the average length of single bonds and that of the adjacent multiple (double or triple) bonds in  $\pi$ -delocalized systems (D- $\pi$ -A). More the bond length alternation (BLA) in the  $\pi$ -conjugated system higher is the perturbation of charges leading to an effective charge transfer between donor and acceptor end groups which

influence the NLO behaviour. In the systems under study (dyes **1-5**) two different donors, morpholine and substituted pyrrole are involved. From the Figures 5 to 7 and Table S2 is seen that morpholine nitrogen is in plane with the  $\pi$ -conjugated system thus expected to involve effectively in charge transfer characteristics. The extent of charge transfer characteristics can be relatively evaluated by observing BLA in DMSO. Thus we considered two D- $\pi$ -A conjugated systems for each of the dye under study as shown in Table S3.

The  $\pi$ -conjugated system originates from the morpholine donor is labelled as a-b-c-d-e (or a-e) for the dyes **1-4** and as a-b-c-d-e-f-g-h-i (or a-i) for the dye **5**, and that originates from the pyrrole donor is labelled as a'-b'-c-d-e (or a'-i) for the dyes **1-4** and as a'-b'-c-d-e-f-g-h-I (or a'-i) for the dye **5**. The lengths of the bonds involved in the D- $\pi$ -A conjugated systems are summarized in Table S3. BLA for the two different D- $\pi$ -A conjugated systems of the dyes **1-5** in  $S_0$  and  $S_1$  states in DMSO media are estimated and summarized in Table S4. Table S4 reveals that in  $S_0$  (GS) there is relatively higher alternation of the bond length among the D- $\pi$ -A conjugated system in which pyrrole donor is effectively involved (that is a' to e or a' to i) compared to the morpholine donor. This confirms the involvement of the pyrrole donor in the effective ICT characteristics, thus the pyrrole substituent is expected to contribute more to enhance the second harmonic generation NLO properties of the push-pull chromophores. Also the BLA in GS for the D- $\pi$ -A conjugated system which originates from the pyrroles donor (a' to e or a' to i) (Table S4) follow similar trend as that of the values of the  $\beta_{CT}$  for dyes **1-5** in DMSO (Table 3).

### 3.6.3. TD-DFT Vertical excitations and vertical emissions of the dyes **1-5**:

The vertical excitation and emission energies, major configurations, and transition nature of the selected  $S_0$  and  $S_1$  states with large oscillator strengths ( $f$ ) of the dyes **1-5** in different solvent media are listed in Table 4. Table 4 reveals that the TD-DFT vertical excitations follow a similar trend as that of experimental absorption maximum values for the dyes under study. For dyes **1-5** in all the solvents studied (Table 4) the vertical excitations originates from the HOMO to LUMO with appreciable orbital contributions.

<<Please insert Table 4 here>>

Vertical excitation values for dye **1** are centered on 408.5 nm to 411.2 nm in various solvents and shows positive effect of increased solvent polarity suggesting decrease of HOMO-LUMO band gap with increase in solvent polarity. The vertical excitation values of dye **2** also shows the similar trend as that of dye **1** and are centered on 408.9 nm to 413.1 nm. TD-DFT calculates the vertical excitation values for the dyes **3** and **4** and surprisingly they are very close to the absorption maximum values in respective solvents. For the dye **5** vertical excitations are centered around 532.5 nm to 538.1 nm in solvents of various polarities (Table 4). Excited ( $S_1$ ) state optimized geometries of the dyes **1-5** in different solvents were subjected to single point energy calculations to get more insight on emission characteristics and results are collected in Table 4. The calculated emissions of the dyes **1-5** are constituted of LUMO→HOMO transitions with good oscillator strengths and orbital contributions.

3.6.4. *Frontier Molecular Orbitals (FMOs) of the push-pull chromophores (dyes 1-5):*

In order to gain detailed information about photophysical behavior of all the molecules under study, it is vital to further examine the frontier molecular orbitals (FMOs), particularly the HOMO-1, HOMO, LUMO and LUMO+1). The contour plots of the HOMO-1, HOMO, LUMO and LUMO+1 of the dyes **1-5** are shown in Figure 8 and energy gaps between HOMO and LUMO for the dyes **1-5** are shown in Figure S11 and collected in Table S5 (ESI).

<<Please insert Figure 8 here>>

<<Please insert Figure 9 here>>

Figure 8 reveals that as expected both the dyes **1** and **2** have similar FMOs (HOMO-1, HOMO, LUMO and LUMO+1). In HOMO-1 of the dyes **1** and **2**, the electron density is mainly localized on pyrrole moiety and partly on thiazole spacer but away from the acceptor ends. In HOMO of the dyes **1** and **2** the electron density is transferred and localized mainly on spacer thiazole.

From Figure 8, it can be seen that the electron density is shared mainly by acceptor end with little on spacer counterpart leaving both the donors with no electron clouds in LUMO. In LUMO+1 again the electron density is completely localized on pyrrole ring leaving rest of the system with no electron density at all supports the involvement of pyrrole as an effective donor in push-pull chromophore. Localization of FMOs in dyes **3** and **4** is bit different than dyes **1** and **2**, the HOMO-1 is mainly localized on the acceptor, particularly on benzimidazole and benzthiazole moiety of the dyes **3** and **4**, respectively, and with little on spacer thiazole.

The HOMO is mainly contributed by the donor morpholine and a spacer thiazole with little on acceptor counterpart but away from the pyrrole. The LUMO is constituted by acceptor counterpart with little on spacer thiazole leaving rest of the system with no electron density. Like dyes **1** and **2** in LUMO+1 the electron density is localized on pyrrole moiety proves its involvement as a donor in push-pull chromophore but here it is partly shared by benzimidazole and benzthiazole counterparts of the acceptor end of the dyes **3** and **4**, respectively. In the dye **5**, HOMO-1 is localized on spacer and acceptor end whereas HOMO is mainly localized on donor morpholine and spacer thiazole. The electron density on donor and spacer in HOMO is transferred to the acceptor end in LUMO whereas LUMO+1 is localized on pyrrole and partly on spacer thiazole and acceptor end to some extent, again confirms the participation of the pyrrole ring in intramolecular charge transfer characteristics.

Figure S11 and Table S5 (ESI) reveals that the dye **1** among the dyes under investigation possess highest HOMO-LUMO band gap in all the solvents studied, thus results in to the higher energy vertical excitation. The dye **2** in various solvents possess slightly lower band gaps compared to the dye **1** and shows absorption maxima shifted to red side (Table 4). The dyes **3** and **4** show considerable lowering of HOMO-LUMO band gaps relative to the dyes **1** and **2**, thus showing pronounced red shift in absorption maxima in various solvent. But between dyes **3** and **4**, the dye **4** show lower HOMO-LUMO band gap energies and hence show red shifted absorption compared to that of the dye **3**. The dye **5**, owing to its increased length of  $\pi$ -conjugation, has got lowest HOMO-LUMO band gap energies among the dyes **1-5**

(Table S5), hence show the highest values of vertical excitation wavelengths (Table 4).

#### 4. Conclusions

Thus, series of novel push-pull chromophores are designed and synthesized and their linear and non-linear optical properties are extensively studied. The observed properties such as photophysical and hyperpolarizability of the dyes are systematically characterized by means of DFT and TD-DFT at B3LYP/6-31G(d) level of theory and the method is found to be very useful and reliable tool for assessing the linear and non-linear optical properties of the chromophores, **1-5**. From the non-linear optical properties particularly good values of second polarizabilities ( $\beta_{CT}$ ) and high thermal stabilities ( $T_d$ ), it can be concluded that the dyes **1-5** can be used as potential NLO materials. The present investigations will be very useful in future design and development of effective and thermally stable organic NLO materials. BLA and Mulliken-Hush analysis results are in correlation with the observed values of  $\beta_{CT}$ . Thus present investigations will be very useful in design and development of potential organic NLO materials.

#### 5. Acknowledgments

One of the authors, KGT, is thankful to the Council of Scientific and Industrial Research (CSIR), India for Junior and Senior Research Fellowships.

**Electronic Supplementary Information (ESI) available**

[Geometry optimization and Energy level tables, absorption emission spectra,  $^1\text{H}$ ,  $^{13}\text{C}$  and HRMS/LCMS spectra are included in supplementary information].

**6. References**

- [1] D.R. Kanis, M.A. Ratner, T.J. Marks, Design and construction of molecular assemblies with large second-order optical nonlinearities. Quantum chemical aspects, *Chem. Rev.* 94 (1994) 195–242. doi:10.1021/cr00025a007.
- [2] S.R. Marder, J.W. Perry, Molecular materials for second-order nonlinear optical applications, *Adv. Mater.* 5 (1993) 804–815. doi:10.1002/adma.19930051104.
- [3] T.J. Marks, M.A. Ratner, Design, Synthesis, and Properties of Molecule-Based Assemblies with Large Second-Order Optical Nonlinearities, *Angew. Chemie Int. Ed. English.* 34 (1995) 155–173. doi:10.1002/anie.199501551.
- [4] L.R. Dalton, A.W. Harper, R. Ghosn, W.H. Steier, M. Ziari, H. Fetterman, et al., Synthesis and Processing of Improved Organic Second-Order Nonlinear Optical Materials for Applications in Photonics, *Chem. Mater.* 7 (1995) 1060–1081. doi:10.1021/cm00054a006.
- [5] Y.-F. Zhou, D.-Q. Yuan, B.-L. Wu, R.-H. Wang, M.-C. Hong, Design of metal-organic NLO materials: complexes derived from pyridine-3,4-dicarboxylate, *New J. Chem.* 28 (2004) 1590. doi:10.1039/b401802h.
- [6] S.A.M. Britto Dhas, S. Natarajan, Growth and characterization of L-prolinium tartrate – A

- new organic NLO material, *Cryst. Res. Technol.* 42 (2007) 471–476.  
doi:10.1002/crat.200610850.
- [7] S.R. Marder, Organic nonlinear optical materials: where we have been and where we are going., *Chem. Commun. (Camb)*. (2006) 131–4. doi:10.1039/b512646k.
- [8] M. Ahlheim, M. Barzoukas, P. V. Bedworth, M. Blanchard-Desce, A. Fort, Z.-Y. Hu, et al., Chromophores with Strong Heterocyclic Acceptors: A Poled Polymer with a Large Electro-Optic Coefficient, *Science (80-. )*. 271 (1996) 335–337.  
doi:10.1126/science.271.5247.335.
- [9] G.S. He, L.-S. Tan, Q. Zheng, P.N. Prasad, Multiphoton absorbing materials: molecular designs, characterizations, and applications., *Chem. Rev.* 108 (2008) 1245–330.  
doi:10.1021/cr050054x.
- [10] R.D. Miller, E.A. Chandross, Introduction: Materials for Electronics, *Chem. Rev.* 110 (2010) 1–2. doi:10.1021/cr900384b.
- [11] S.R. Forrest, M.E. Thompson, Introduction: Organic Electronics and Optoelectronics, *Chem. Rev.* 107 (2007) 923–925. doi:10.1021/cr0501590.
- [12] S. Kato, F. Diederich, Non-planar push-pull chromophores., *Chem. Commun. (Camb)*. 46 (2010) 1994–2006. doi:10.1039/b926601a.
- [13] S.R. Marder, L.-T. Cheng, B.G. Tiemann, The first molecular electronic hyperpolarizabilities of highly polarizable organic molecules: 2,6-di-tert-butylindoanilines, *J. Chem. Soc. Chem. Commun.* (1992) 672.  
doi:10.1039/c39920000672.
- [14] S.R. Marder, C.B. Gorman, B.G. Tiemann, L.T. Cheng, Stronger acceptors can diminish nonlinear optical response in simple donor-acceptor polyenes, *J. Am. Chem. Soc.* 115

- (1993) 3006–3007. doi:10.1021/ja00060a071.
- [15] J. Kulhánek, F. Bureš, Imidazole as a parent  $\pi$ -conjugated backbone in charge-transfer chromophores., *Beilstein J. Org. Chem.* 8 (2012) 25–49. doi:10.3762/bjoc.8.4.
- [16] C.G. Bethea, Experimental technique of dc induced SHG in liquids: measurement of the nonlinearity of CH(2)I(2)., *Appl. Opt.* 14 (1975) 1447–51. doi:10.1364/AO.14.001447.
- [17] C. Bosshard, G. Knoopfle, P. Preitre, P. Gunter, Second-order polarizabilities of nitropyridine derivatives determined with electric-field-induced second-harmonic generation and a solvatochromic method: A comparative study, *J. Appl. Phys.* 71 (1992) 1594. doi:10.1063/1.351237.
- [18] M.S. Paley, J.M. Harris, H. Looser, J.C. Baumert, G.C. Bjorklund, D. Jundt, et al., A solvatochromic method for determining second-order polarizabilities of organic molecules [Erratum to document cited in CA111(11):96600e], *J. Org. Chem.* 55 (1990) 1692–1692. doi:10.1021/jo00292a057.
- [19] E. Baltazzi, L.I. Krimen, Recent Advances in the Chemistry of Pyrrole., *Chem. Rev.* 63 (1963) 511–556. doi:10.1021/cr60225a004.
- [20] B.A. Trofimov, Prospects for the chemistry of pyrrole, *Russ. Chem. Rev.* 58 (1989) 967–976. doi:10.1070/RC1989v058n10ABEH003489.
- [21] A. Loudet, K. Burgess, BODIPY dyes and their derivatives: syntheses and spectroscopic properties., *Chem. Rev.* 107 (2007) 4891–932. doi:10.1021/cr078381n.
- [22] B. Milián, E. Ortí, V. Hernández, J.T. López Navarrete, T. Otsubo, Spectroscopic and Theoretical Study of Push–Pull Chromophores Containing Thiophene-Based Quinonoid Structures as Electron Spacers, *J. Phys. Chem. B.* 107 (2003) 12175–12183. doi:10.1021/jp0354651.

- [23] N. Ghoneim, Photophysics of Nile red in solution: Steady state spectroscopy, *Spectrochim. Acta Part A Mol. Biomol. Spectrosc.* 56 (2000) 1003–1010.  
doi:10.1016/S1386-1425(99)00199-7.
- [24] R. Sens, K.H. Drexhage, Fluorescence quantum yield of oxazine and carbazine laser dyes, *J. Lumin.* 24–25 (1981) 709–712. doi:10.1016/0022-2313(81)90075-2.
- [25] M.J. Frisch, G.W. Trucks, H.B. Schlegel, G.E. Scuseria, M.A. Robb, J.R. Cheeseman, et al., *Gaussian 09 C.01*, Gaussian Inc., Wallingford CT, 2009.
- [26] O. Treutler, R. Ahlrichs, Efficient molecular numerical integration schemes, *J. Chem. Phys.* 102 (1995) 346. doi:10.1063/1.469408.
- [27] A.D. Becke, A new mixing of Hartree–Fock and local density-functional theories, *J. Chem. Phys.* 98 (1993) 1372. doi:10.1063/1.464304.
- [28] R.G. Lee, Chengteh and Yang, Weitao and Parr, Development of the Colle-Salvetti correlation-energy formula into a functional of the electron density, *Phys. Rev. B.* 37 (1988) 785–789. doi:10.1103/PhysRevB.37.785.
- [29] W.J. Hehre, Ab initio molecular orbital theory, *Acc. Chem. Res.* 9 (1976) 399–406.  
doi:10.1021/ar50107a003.
- [30] R. Bauernschmitt, R. Ahlrichs, Treatment of electronic excitations within the adiabatic approximation of time dependent density functional theory, *Chem. Phys. Lett.* 256 (1996) 454–464. doi:10.1016/0009-2614(96)00440-X.
- [31] F. Furche, D. Rappoport, *Computational Photochemistry* (Google eBook), Elsevier, Amsterdam, 2005.  
<http://books.google.com/books?hl=en&lr=&id=Eams0jTx9foC&pgis=1> (accessed March 17, 2014).

- [32] Y. Gabe, T. Ueno, Y. Urano, H. Kojima, T. Nagano, Tunable design strategy for fluorescence probes based on 4-substituted BODIPY chromophore: improvement of highly sensitive fluorescence probe for nitric oxide., *Anal. Bioanal. Chem.* 386 (2006) 621–6. doi:10.1007/s00216-006-0587-y.
- [33] F. Furche, R. Ahlrichs, Adiabatic time-dependent density functional methods for excited state properties, *J. Chem. Phys.* 117 (2002) 7433. doi:10.1063/1.1508368.
- [34] J. Leszczynski, M. Shukla, eds., *Practical Aspects of Computational Chemistry: Methods, Concepts and Applications* (Google eBook), Springer, 2009.  
<http://books.google.com/books?id=esOANcsz5w8C&pgis=1> (accessed March 20, 2014).
- [35] G. Scalmani, M.J. Frisch, B. Mennucci, J. Tomasi, R. Cammi, V. Barone, Geometries and properties of excited states in the gas phase and in solution: theory and application of a time-dependent density functional theory polarizable continuum model., *J. Chem. Phys.* 124 (2006) 94107. doi:10.1063/1.2173258.
- [36] K.G. Thorat, H. Bhakhoa, P. Ramasami, N. Sekar, NIR-Emitting Boradiazaindacene Fluorophores -TD-DFT Studies on Electronic Structure and Photophysical Properties., *J. Fluoresc.* 25 (2015) 69–78. doi:10.1007/s10895-014-1481-1.
- [37] K.G. Thorat, P. Kamble, R. Mallah, A.K. Ray, N. Sekar, Congeners of Pyrromethene-567 dye: Perspectives from synthesis, photophysics, photostability, laser and TD-DFT theory., *J. Org. Chem.* 80 (2015) 6152–6164. doi:10.1021/acs.joc.5b00654.
- [38] V. Barone, M. Cossi, Quantum Calculation of Molecular Energies and Energy Gradients in Solution by a Conductor Solvent Model, *J. Phys. Chem. A.* 102 (1998) 1995–2001. doi:10.1021/jp9716997.
- [39] M. Cossi, V. Barone, R. Cammi, J. Tomasi, Ab initio study of solvated molecules: a new

- implementation of the polarizable continuum model, *Chem. Phys. Lett.* 255 (1996) 327–335. doi:10.1016/0009-2614(96)00349-1.
- [40] J. Tomasi, B. Mennucci, R. Cammi, Quantum Mechanical Continuum Solvation Models, *Chem. Rev.* 105 (2005) 2999–3093. doi:10.1021/cr9904009.
- [41] S. Mula, A.K. Ray, M. Banerjee, T. Chaudhuri, K. Dasgupta, S. Chattopadhyay, Design and development of a new pyrromethene dye with improved photostability and lasing efficiency: theoretical rationalization of photophysical and photochemical properties., *J. Org. Chem.* 73 (2008) 2146–54. doi:10.1021/jo702346s.
- [42] A. Souldozi, A. Ramazani, A.R. Dadrass, K. Ślepokura, T. Lis, Efficient One-Pot Synthesis of Alkyl 2-(Dialkylamino)-4-phenylthiazole-5-carboxylates and Single-Crystal X-Ray Structure of Methyl 2-(Diisopropylamino)-4-phenylthiazole-5-carboxylate, *Helv. Chim. Acta.* 95 (2012) 339–348. doi:10.1002/hlca.201100322.
- [43] P.G. Umape, V.S. Patil, V.S. Padalkar, K.R. Phatangare, V.D. Gupta, A.B. Thate, et al., Synthesis and characterization of novel yellow azo dyes from 2-morpholin-4-yl-1,3-thiazol-4(5H)-one and study of their azo–hydrazone tautomerism, *Dye. Pigment.* 99 (2013) 291–298. doi:10.1016/j.dyepig.2013.05.002.
- [44] G. Chennakrishnareddy, H. Debasis, R. Jayan, S.G. Manjunatha, Facile synthesis of 3-aryl/alkylamino 5-aryl/alkyl 1,2,4-oxadiazoles from acylthiourea, *Tetrahedron Lett.* 52 (2011) 6170–6173. doi:10.1016/j.tetlet.2011.09.048.
- [45] M. Sabbaghan, M. Alidoust, Z. Hossaini, A Rapid, Four-Component Synthesis of Functionalized Thiazoles, *Comb. Chem. High Throughput Screen.* 14 (2011) 824–828. doi:10.2174/138620711796957134.
- [46] Z. Zheng, Z. Yu, M. Yang, F. Jin, Q. Zhang, H. Zhou, et al., Substituent group variations

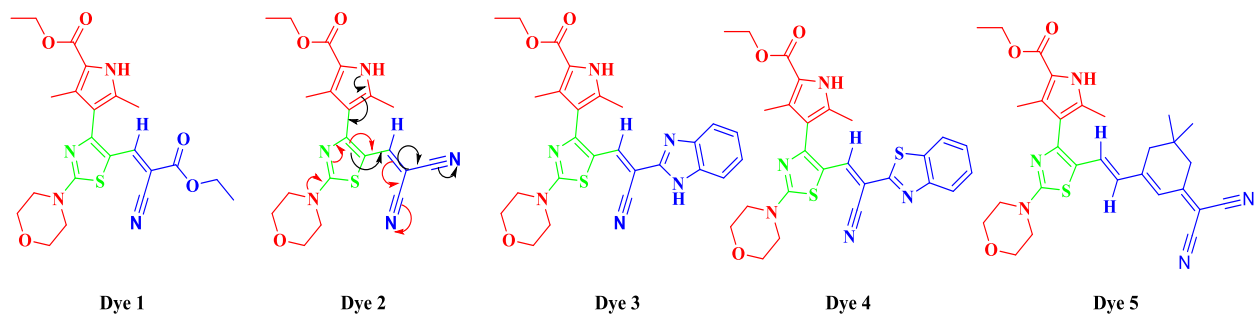
- directing the molecular packing, electronic structure, and aggregation-induced emission property of isophorone derivatives., *J. Org. Chem.* 78 (2013) 3222–34.  
doi:10.1021/jo400116j.
- [47] L. Dell'Amico, G. Rassu, V. Zambrano, A. Sartori, C. Curti, L. Battistini, et al., Exploring the vinylogous reactivity of cyclohexenyliidene malononitriles: switchable regioselectivity in the organocatalytic asymmetric addition to enals giving highly enantioenriched carbabicyclic structures., *J. Am. Chem. Soc.* 136 (2014) 11107–14.  
doi:10.1021/ja5054576.
- [48] B. Valeur, M.N. Berberan-Santos, *Molecular Fluorescence: Principles and Applications*, John Wiley & Sons, 2012.  
<https://books.google.com/books?hl=en&lr=&id=NdySsFt8TN8C&pgis=1> (accessed July 10, 2015).
- [49] M. Józefowicz, J.R. Heldt, Dipole moments studies of fluorenone and 4-hydroxyfluorenone., *Spectrochim. Acta. A. Mol. Biomol. Spectrosc.* 67 (2007) 316–20.  
doi:10.1016/j.saa.2006.07.019.
- [50] G. V. Loukova, A.A. Milov, V.P. Vasiliev, V.A. Smirnov, Dipole moment of a metallocene precatalyst in the ground and excited states, *Russ. Chem. Bull.* 57 (2009) 1166–1171. doi:10.1007/s11172-008-0145-1.
- [51] J. Thipperudrappa, Analysis of Solvent Effect in a Ketocyanine Dye Using Various Solvent Polarity Scales and Estimation of Dipole Moments, *J. Eng. Comput. Appl. Sci.* 3 (2014) 25–32. <http://www.borjournals.com/a/index.php/jecas/article/view/1607> (accessed October 13, 2015).
- [52] B.J. Coe, J. Fielden, S.P. Foxon, J.A. Harris, M. Helliwell, B.S. Brunschwig, et al., Diquat

- derivatives: highly active, two-dimensional nonlinear optical chromophores with potential redox switchability., *J. Am. Chem. Soc.* 132 (2010) 10498–512. doi:10.1021/ja103289a.
- [53] Q. Wang, M.D. Newton, Structure, Energetics, and Electronic Coupling in the (TCNE 2) - • Encounter Complex in Solution: A Polarizable Continuum Study †, *J. Phys. Chem. B.* 112 (2008) 568–576. doi:10.1021/jp0753528.
- [54] R.J. Cave, M.D. Newton, Calculation of electronic coupling matrix elements for ground and excited state electron transfer reactions: Comparison of the generalized Mulliken–Hush and block diagonalization methods, *J. Chem. Phys.* 106 (1997) 9213. doi:10.1063/1.474023.
- [55] M. Rust, J. Lappe, R.J. Cave, Multistate Effects in Calculations of the Electronic Coupling Element for Electron Transfer Using the Generalized Mulliken–Hush Method, *J. Phys. Chem. A.* 106 (2002) 3930–3940. doi:10.1021/jp0142886.
- [56] J. Lappe, R.J. Cave, M.D. Newton, I. V. Rostov, A Theoretical Investigation of Charge Transfer in Several Substituted Acridinium Ions †, *J. Phys. Chem. B.* 109 (2005) 6610–6619. doi:10.1021/jp0456133.
- [57] D. Beljonne, G. Pourtois, M.A. Ratner, J.L. Brédas, Pathways for photoinduced charge separation in DNA hairpins., *J. Am. Chem. Soc.* 125 (2003) 14510–7. doi:10.1021/ja035596f.
- [58] J. Zheng, Y.K. Kang, M.J. Therien, D.N. Beratan, Generalized Mulliken-Hush analysis of electronic coupling interactions in compressed pi-stacked porphyrin-bridge-quinone systems., *J. Am. Chem. Soc.* 127 (2005) 11303–10. doi:10.1021/ja050984y.
- [59] C. Creutz, M.D. Newton, N. Sutin, Metal—ligand and metal—metal coupling elements, *J. Photochem. Photobiol. A Chem.* 82 (1994) 47–59. doi:10.1016/1010-6030(94)02013-2.

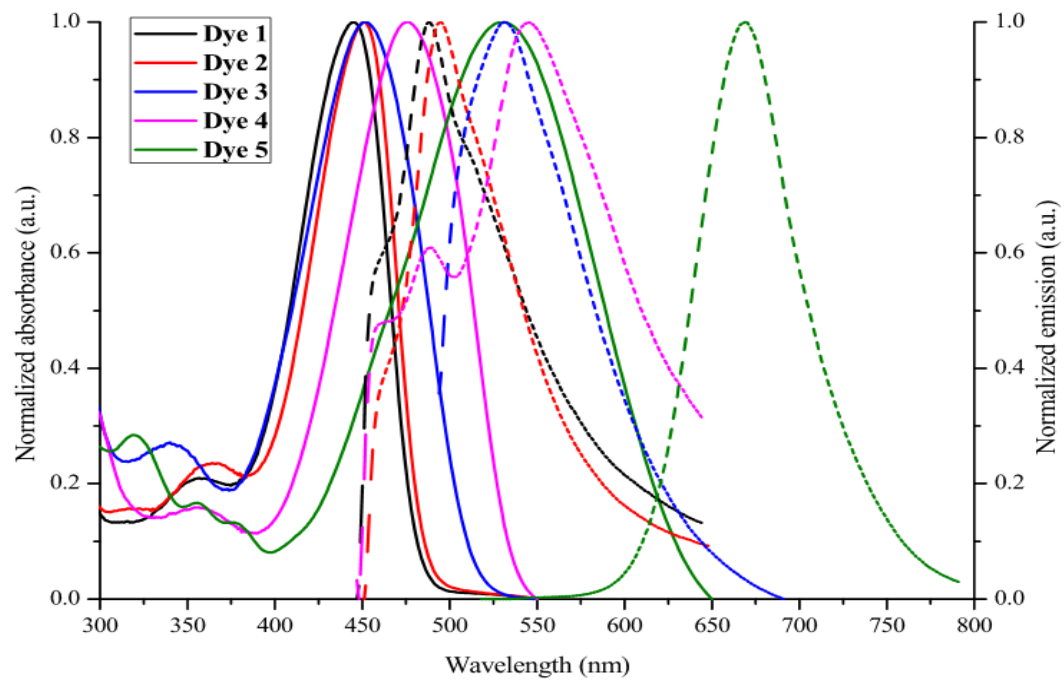
- [60] M.D. Newton, Medium reorganization and electronic coupling in long-range electron transfer, *J. Electroanal. Chem.* 438 (1997) 3–10. doi:10.1016/S0022-0728(96)05025-5.
- [61] M.S. Paley, J.M. Harris, H. Looser, J.C. Baumert, G.C. Bjorklund, D. Jundt, et al., A solvatochromic method for determining second-order polarizabilities of organic molecules, *J. Org. Chem.* 54 (1989) 3774–3778. doi:10.1021/jo00277a007.
- [62] H.-C. Song, Y.-W. Chen, X.-L. Zheng, B.-N. Ying, Study on second harmonic generation of 10-hydrocarbylacridones, *Spectrochim. Acta Part A Mol. Biomol. Spectrosc.* 57 (2001) 1717–1723. doi:10.1016/S1386-1425(01)00394-8.
- [63] A. Abboto, L. Beverina, S. Bradamante, A. Facchetti, C. Klein, G.A. Pagani, et al., A distinctive example of the cooperative interplay of structure and environment in tuning of intramolecular charge transfer in second-order nonlinear optical chromophores., *Chemistry*. 9 (2003) 1991–2007. doi:10.1002/chem.200204356.
- [64] F. Momicchioli, G. Ponterini, D. Vanossi, First- and second-order polarizabilities of simple merocyanines. An experimental and theoretical reassessment of the two-level model., *J. Phys. Chem. A*. 112 (2008) 11861–72. doi:10.1021/jp8080854.
- [65] B. Carlotti, R. Flamini, I. Kikaš, U. Mazzucato, A. Spalletti, Intramolecular charge transfer, solvatochromism and hyperpolarizability of compounds bearing ethynylene or ethynylene bridges, *Chem. Phys.* 407 (2012) 9–19. doi:10.1016/j.chemphys.2012.08.006.
- [66] J.L. Oudar, D.S. Chemla, Hyperpolarizabilities of the nitroanilines and their relations to the excited state dipole moment, *J. Chem. Phys.* 66 (1977) 2664. doi:10.1063/1.434213.
- [67] S. Vidya, C. Ravikumar, I. Hubert Joe, P. Kumaradhas, B. Devipriya, K. Raju, Vibrational spectra and structural studies of nonlinear optical crystal ammonium D, L-tartrate: a density functional theoretical approach, *J. Raman Spectrosc.* 42 (2011) 676–684.

- doi:10.1002/jrs.2743.
- [68] C. Meganathan, S. Sebastian, M. Kurt, K.W. Lee, N. Sundaraganesan, Molecular structure, spectroscopic (FTIR, FTIR gas phase, FT-Raman) first-order hyperpolarizability and HOMO-LUMO analysis of 4-methoxy-2-methyl benzoic acid, *J. Raman Spectrosc.* 41 (2010) 1369–1378. doi:10.1002/jrs.2562.
- [69] R.J. Jeng, Y.M. Chen, A.K. Jain, J. Kumar, S.K. Tripathy, Second order optical nonlinearity on a modified sol-gel system at 100.degree.C, *Chem. Mater.* 4 (1992) 972–975. doi:10.1021/cm00023a006.
- [70] W.-J. Kuo, G.-H. Hsiue, R.-J. Jeng, Novel Guest–Host NLO Poly(ether imide) Based on a Two-Dimensional Carbazole Chromophore with Sulfonyl Acceptors, *Macromolecules.* 34 (2001) 2373–2384. doi:10.1021/ma0017485.
- [71] L. Chen, Y. Cui, X. Mei, G. Qian, M. Wang, Synthesis and characterization of triphenylamino-substituted chromophores for nonlinear optical applications, *Dye. Pigment.* 72 (2007) 293–298. doi:10.1016/j.dyepig.2005.09.008.
- [72] K.G. Thorat, A.K. Ray, N. Sekar, Modulating TICT to ICT characteristics of acid switchable red emitting boradiazaindacene chromophores: Perspectives from synthesis, photophysical, hyperpolarizability and TD-DFT studies, *Dye. Pigment.* 136 (2017) 321–334. doi:10.1016/j.dyepig.2016.08.049.
- [73] S.S. Patil, K.G. Thorat, R. Mallah, N. Sekar, Novel Rhodafluors: Synthesis, Photophysical, pH and TD-DFT Studies, *J. Fluoresc.* (2016) 1–11. doi:10.1007/s10895-016-1915-z.

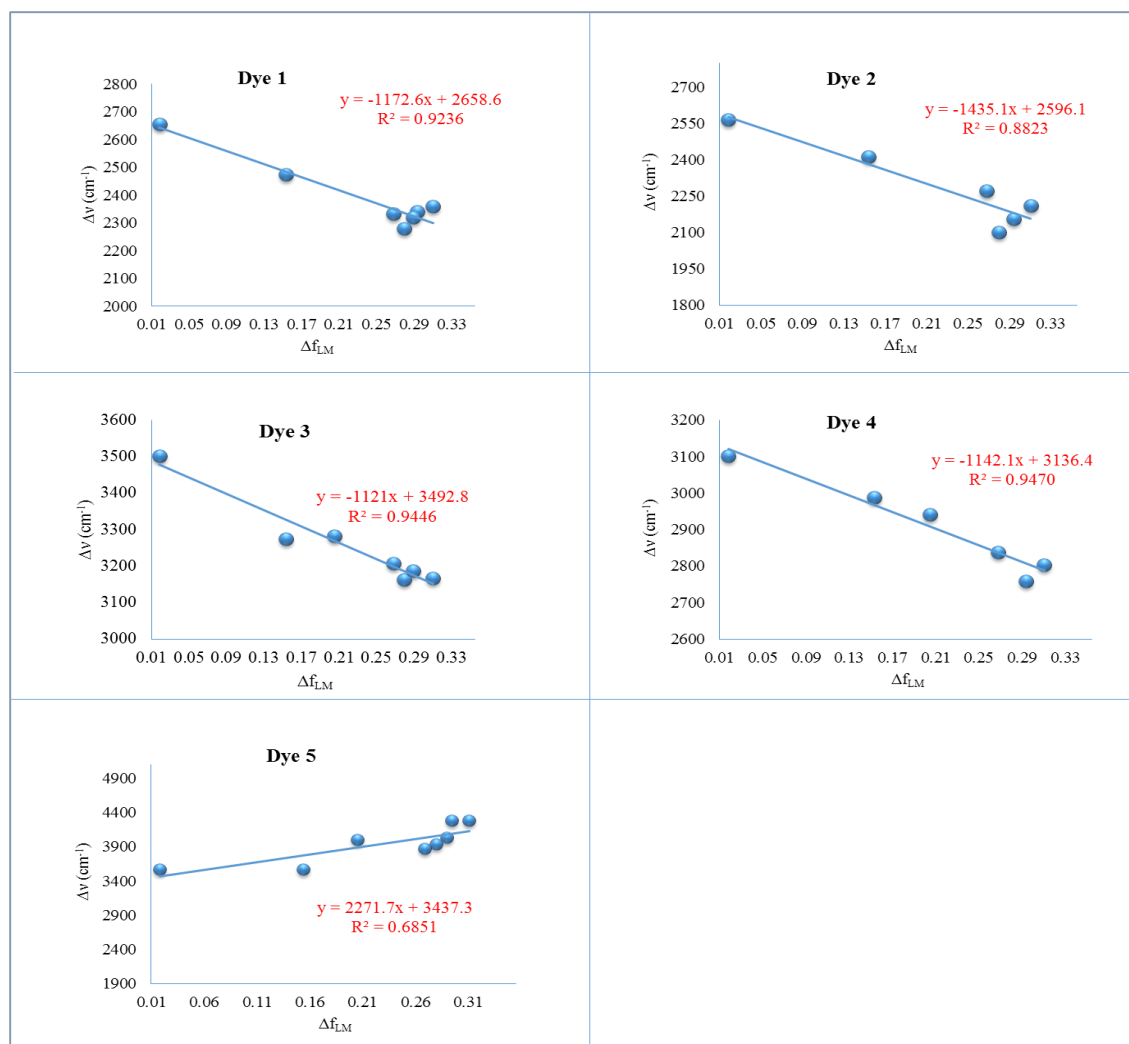
## List of Figures



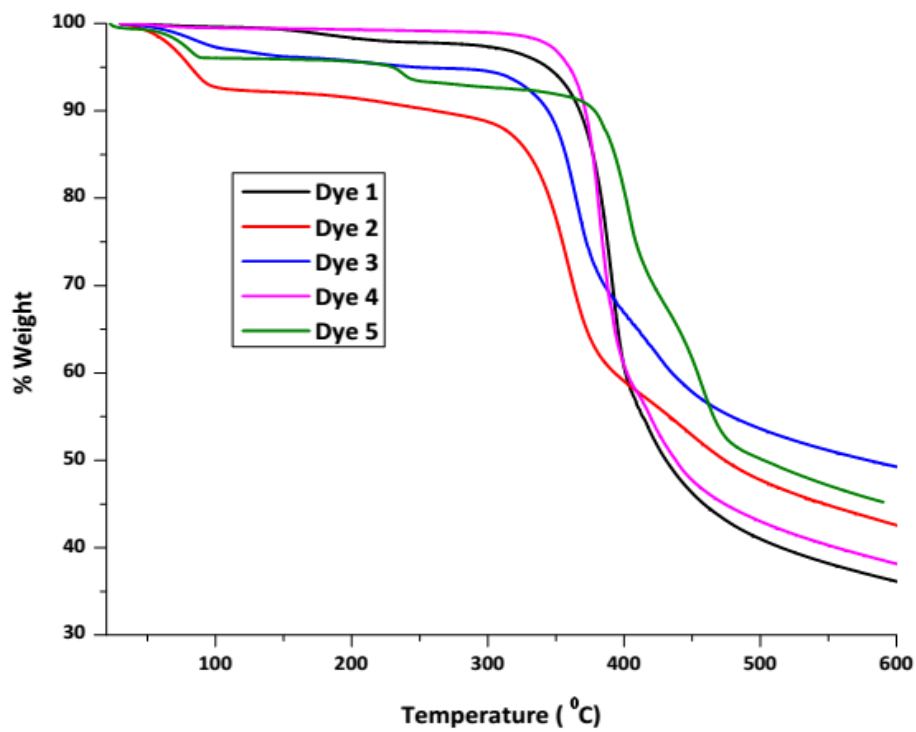
**Figure 1.** Molecular structures of the push-pull chromophores, **1-5**, under study (Arrows on fluorophore **2** represents the possibilities of movement of  $\pi$ -electrons clouds from donors (from pyrrole-black arrows and from morpholine-red arrows) to acceptor).



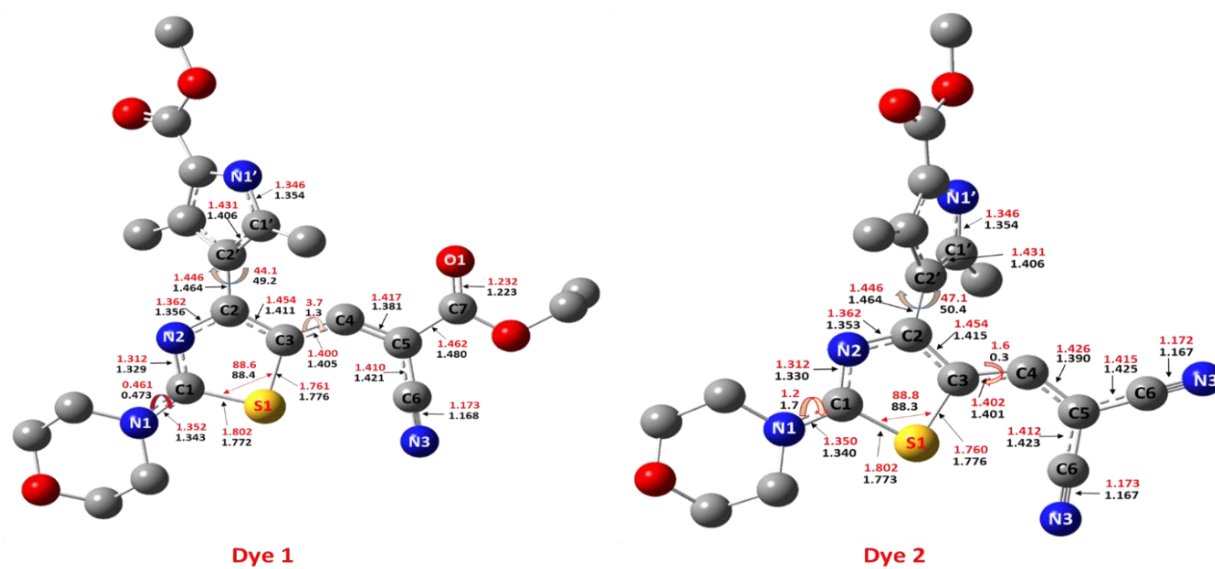
**Figure 2.** Normalized absorption (solid lines) and emission (dashed lines) spectra of the dyes **1-5** in DMSO



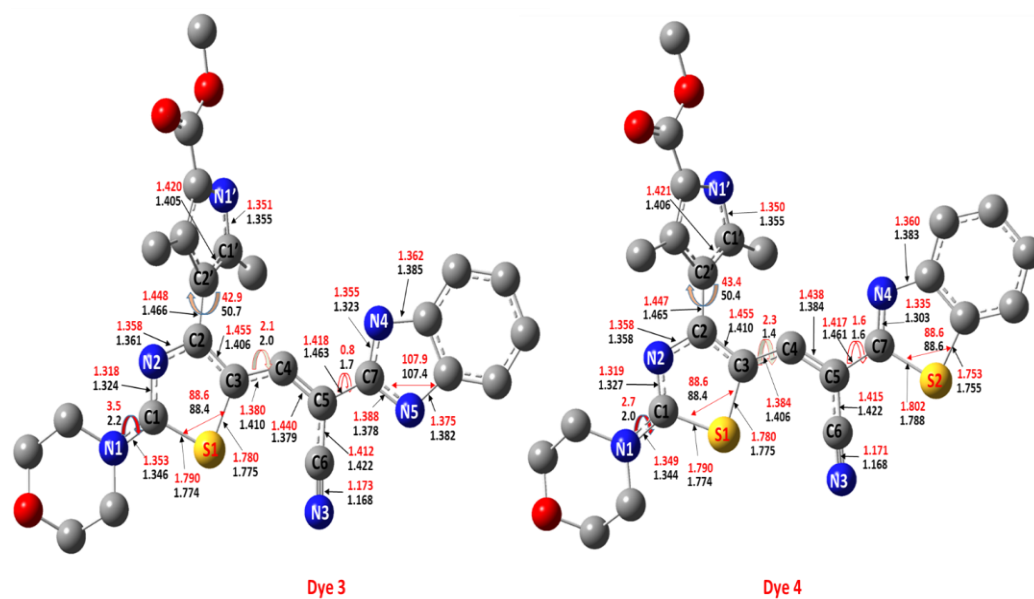
**Figure 3.** Plots of Lippert-Mataga solvent polarity function ( $\Delta f_{LM}$ ) versus Stokes shift ( $\Delta\nu$ ) for the dyes 1-5 (plots A to E, respectively)



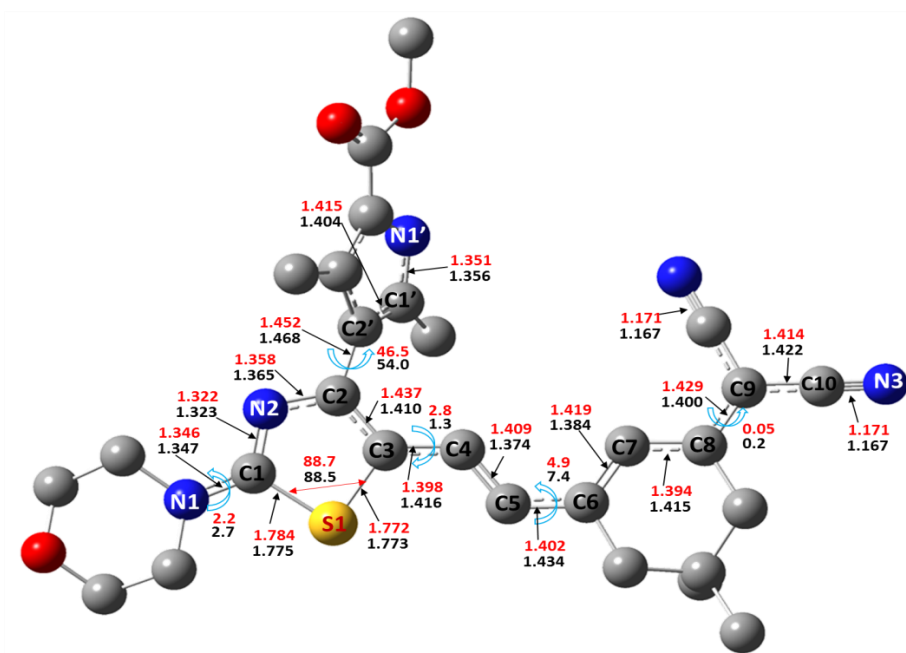
**Figure 4.** Thermogravimetry analysis (TGA) curves of the dyes **1-5**



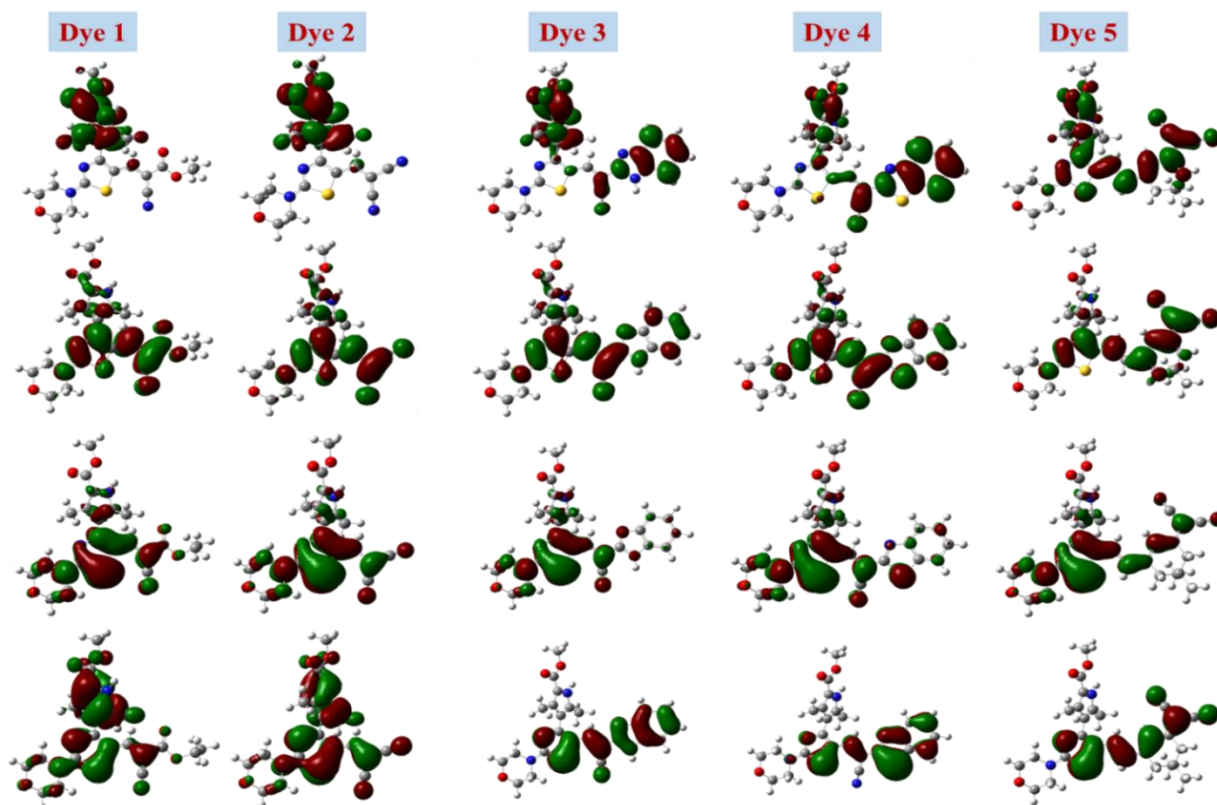
**Figure 5.** TD-DFT (B3LYP/6-31G(d)) optimized geometries of the dyes **1** and **2**, and ground (black digits) and excited (red digits) geometrical parameters (bond lengths are in Å, dihedral angles are in degree °) in DMSO.



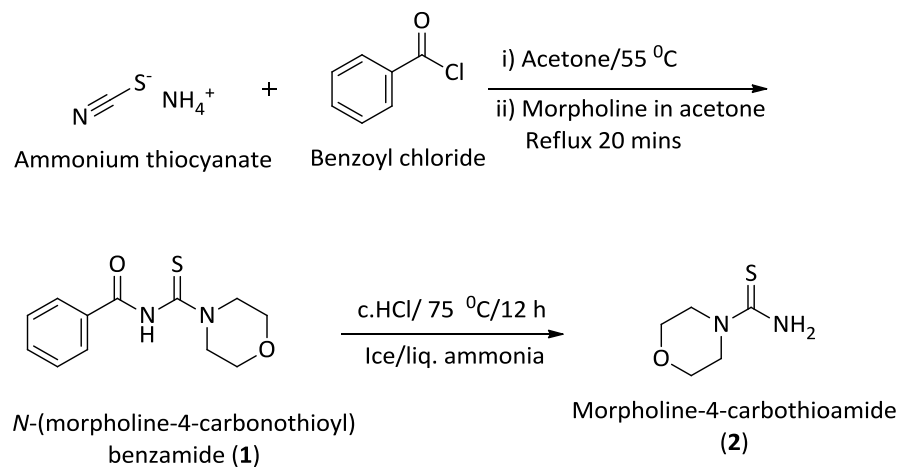
**Figure 6.** TD-DFT (B3LYP/6-31G(d)) optimized geometries of the dyes **3** and **4**, and ground (black digits) and excited (red digits) geometrical parameters (bond lengths are in Å, dihedral angles are in degree °) in DMSO

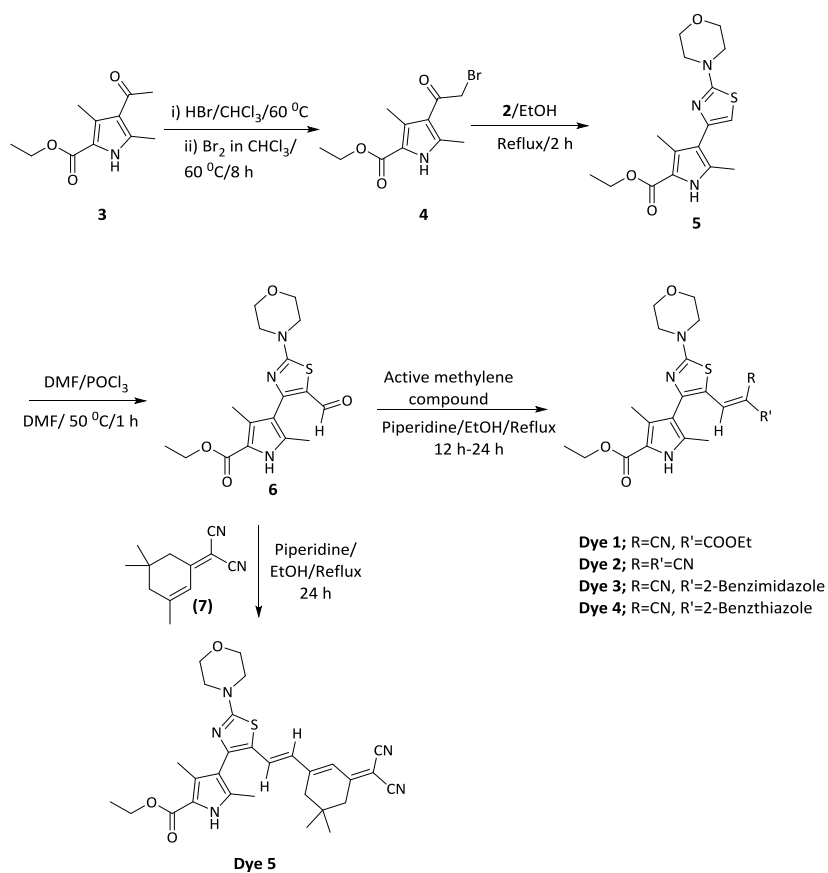


**Figure 7.** TD-DFT (B3LYP/6-31G(d)) optimized geometries of the dye **5**, and ground (black digits) and excited (red digits) geometrical parameters (bond lengths are in Å, dihedral angles are in degree °) in DMSO.



**Figure 8.** Energy level and electron density distribution of frontier molecular orbitals (From top to bottom= LUMO+1, LUMO, HOMO and HOMO-1, respectively) of dyes **1-5** in DMSO solvent, calculated by B3LYP/6-31G(d)level of theory (The orbital diagrams are plotted with the contour value of 0.02 a. u.)

**List of Schemes****Scheme 1.** Synthesis of thiourea intermediate (**2**)



**Scheme 2.** Synthesis of novel pyrrole based styryl derivatives (dyes 1-5)

**Table 1.** Photophysical properties of the push pull fluorophores (dyes **1-5**) in various solvent

Solvent	$\lambda_{\text{abs}}^{[a]}$ nm	Fwhm <sup>[b]</sup>		$\lambda_{\text{em}}^{[c]}$ nm	Fwhm <sup>[d]</sup>		$\Delta\nu^{[e]}$		$\epsilon_{\text{max}}^{[f]}$ M <sup>-1</sup> cm <sup>-1</sup>	$\phi_{\text{f}}^{[g]}$
		nm	cm <sup>-1</sup>		nm	cm <sup>-1</sup>	nm	cm <sup>-1</sup>		
<b>Dye 1</b>										
DMSO	447	58.4	3062	499	67.5	2726	52	2331	45340	0.026
DMF	444	59.0	3146	491	57.4	2313	47	2156	43464	0.056
MeCN	433	59.5	3290	486	58.9	2424	53	2519	47810	0.053
MeOH	436	62.7	3471	494	61.1	2457	58	2693	28029	0.045
EtOH	438	62.5	3433	488	64.2	2537	50	2339	21741	0.049
Acetone	433	58.6	3221	494	77.7	3282	61	2852	47240	0.009
EtOAc	441	57.9	3235	490	60.8	3260	49	2268	43556	0.018
CHCl <sub>3</sub>	434	57.8	3190	492	68.2	2806	58	2716	44197	0.094
Toluene	432	58.3	3254	488	52.9	2109	56	2656	46850	0.013
<b>Dye 2</b>										
DMSO	453	55.4	2827	505	54.2	2074	52	2273	44690	0.006
DMF	450	55.9	2901	494	62.0	2445	44	1979	41427	0.017
MeCN	438	56.4	3026	488	60.8	2454	50	2339	44946	0.017
MeOH	438	59.2	3189	497	60.9	2347	59	2710	23831	0.019
EtOH	443	58.2	3107	491	59.8	2310	48	2207	13262	0.013
Acetone	439	55.9	2984	494	51.4	1969	55	2536	45327	0.006
EtOAc	439	55.7	3027	498	52.6	2056	59	2699	33537	0.005
CHCl <sub>3</sub>	443	54.3	2908	497	54.0	2123	54	2453	44121	0.020
Toluene	440	55.4	3003	495	54.2	2159	55	2525	24231	0.008
<b>Dye 3</b>										
DMSO	453	78.5	3925	533	92.2	3145	80	3313	23077	0.017
DMF	453	78.5	4011	523	96.6	3399	70	2955	26110	0.036
MeCN	445	77.5	4053	518	98.3	3415	73	3167	26133	0.022
MeOH	467	83.9	4382	535	87.0	3059	68	3338	24772	0.021
EtOH	469	85.4	4469	539	89.2	3129	70	2769	22527	0.018
Acetone	450	77.7	4027	528	93.0	3192	78	3283	27079	0.009
EtOAc	449	77.7	4029	526	92.9	3194	77	3260	24952	0.006
CHCl <sub>3</sub>	456	78.9	3959	536	89.8	3001	80	3273	26289	0.026
Toluene	452	79.0	3962	537	92.9	3097	85	3502	23444	0.006

**Dye 4**

DMSO	478	79.9	3582	551	79.8	2585	73	2772	40262	0.008
DMF	466	79.8	3640	535	76.1	2475	69	2768	42000	0.013
MeCN	476	79.9	3801	543	79.5	2651	67	2592	45581	0.007
MeOH	465	80.6	3863	543	76.3	2517	78	3089	37008	0.008
EtOH	470	81.3	3871	537	75.3	2472	67	2655	13939	0.006
Acetone	466	78.6	3697	542	80.9	2668	76	3009	43973	0.003
EtOAc	463	78.2	3727	545	82.3	2709	82	3250	40093	0.002
CHCl <sub>3</sub>	465	77.3	3695	543	80.8	2645	78	3089	45272	0.010
Toluene	464	78.2	3719	542	83.7	2733	78	3102	29710	0.003

**Dye 5**

DMSO	535	123.6	4510	670	68.2	1513	135	3766	49398	0.037
DMF	528	124.6	4689	664	68.3	1540	136	3879	51254	0.034
MeCN	509	107.2	4292	657	67.2	1563	148	4426	45208	0.021
MeOH	501	118.7	4910	659	68.5	1581	158	4786	53360	0.036
EtOH	510	120.8	4823	657	69.4	1604	147	4387	52802	0.043
Acetone	507	120.4	4753	639	69.5	1627	132	4074	49000	0.042
EtOAc	515	110.9	4498	650	79.9	1935	135	4033	41983	0.029
CHCl <sub>3</sub>	520	113.6	4461	634	83.8	2045	114	3458	46025	0.041
Toluene	507	101.6	4106	619	94.8	2395	112	3569	42716	0.039

<sup>[a]</sup>Experimental absorption maxima; <sup>[b]</sup>Full width at half absorption maxima; <sup>[c]</sup>Experimental emission maxima; <sup>[d]</sup>Full width at half emission maxima; <sup>[e]</sup>Stokes shift; <sup>[f]</sup>Molar extinction coefficient at absorption maxima; <sup>[g]</sup>Quantum yield of fluorescence determined using Nile red in ethanol ( $\phi_{fl}=0.12$ ) for dyes **1-4** and Nile blue-a perchlorate in ethanol ( $\phi_{fl}=0.27$ ) for the dye **5**.

**Table 2.** Linear optical and charge transfer characteristics of the dyes **1-5** in different microenvironments

Solvent	$a^{[a]}$ /10 <sup>-8</sup> cm	$\int \varepsilon(\vartheta) d\nu^{[b]}$ /10 <sup>7</sup> M <sup>-1</sup> cm <sup>-2</sup>	$f^{[c]}$ e.s.u	$\mu_{ge}^{[d]}$ /10 <sup>-18</sup> e.s.u	$\Delta\mu_{CT}^{[e]}$ /10 <sup>-18</sup> e.s.u	$\Delta\mu_{ge}^{[f]}$ /10 <sup>-17</sup> e.s.u	$C_b^{2[g]}$	$H_{DA}^{[h]}$ cm <sup>-1</sup>	$R_{DA}^{[i]}$ Å
<b>Dye 1</b>									
DMSO	3.16	1.50	0.4451	6.51	1.93	1.32	0.427	11066	3.28
MeOH	3.14	1.18	0.3900	6.02	1.90	1.22	0.422	11328	2.72
CHCl <sub>3</sub>	3.13	1.51	0.4585	6.51	1.89	1.32	0.428	11401	3.26
Toluene	3.18	1.19	0.3490	5.67	1.94	1.15	0.416	11409	3.39
<b>Dye 2</b>									
DMSO	3.03	1.27	0.3769	6.03	2.00	1.22	0.418	10889	3.16
MeOH	3.07	1.17	0.3867	6.00	2.03	1.22	0.417	11256	2.41
CHCl <sub>3</sub>	3.07	1.29	0.4372	6.42	2.03	1.24	0.418	11134	3.21
Toluene	3.07	1.15	0.1320	3.52	2.03	0.73	0.362	10919	2.43
<b>Dye 3</b>									
DMSO	3.27	1.21	0.3888	6.13	1.95	1.24	0.421	10900	2.67
MeOH	3.26	1.11	0.3668	5.90	1.96	1.20	0.418	11059	2.84
CHCl <sub>3</sub>	3.24	1.15	0.3492	5.82	1.94	1.18	0.418	10816	2.88
Toluene	3.14	0.97	0.2845	5.23	1.86	1.06	0.413	10892	2.71
<b>Dye 4</b>									
DMSO	3.32	1.56	0.4629	6.86	2.05	1.39	0.426	10346	3.46
MeOH	3.22	1.35	0.4461	6.65	1.94	1.35	0.428	10640	3.39
CHCl <sub>3</sub>	3.31	1.74	0.5283	7.23	2.03	1.46	0.431	10649	3.67
Toluene	3.22	1.14	0.3343	5.75	1.94	1.17	0.417	10626	2.99
<b>Dye 5</b>									
DMSO	3.40	2.36	0.7004	8.93	3.00	1.81	0.417	9217	4.56
MeOH	3.31	2.71	0.8956	9.77	2.86	1.98	0.428	9875	4.77
CHCl <sub>3</sub>	3.40	2.31	0.7014	8.81	2.98	1.79	0.417	9481	4.32
Toluene	3.24	1.59	0.4663	7.09	2.77	1.45	0.404	9680	3.96

<sup>[a]</sup>Onsager radius; <sup>[b]</sup>Integrated area of absorption coefficient; <sup>[c]</sup>Oscillator strength; <sup>[d]</sup>Transition dipole moment; <sup>[e]</sup>Difference between ground and excited state dipole moments evaluated using Lippert-Mataga solvent polarity parameter; <sup>[f]</sup>Dipole moment change between the diabatic states; <sup>[g]</sup>Degree of delocalization; <sup>[h]</sup>Electronic coupling matrix/Strength of electronic coupling between the ground ( $S_0$ ) and charge transfer excited states; <sup>[i]</sup>Donor acceptor separation.

**Table 3.** Measured and TD-DFT (B3LYP/6-31G(d), CAM- B3LYP/6-31G(d) and BHHLYP/6-31G(d) methods) linear and non-linear optical properties of the dyes **1-5** in different microenvironments

	Solvent	$\mu^{[a]}$ /10 <sup>-17</sup> e.s.u	$\alpha_{CT}^{[b]}$ /10 <sup>-23</sup> e.s.u	$\alpha_0^{[c]}$ /10 <sup>-23</sup> e.s.u	$\beta_{CT}^{[d]}$ /10 <sup>-30</sup> e.s.u	$(\beta_0)^{[e]}$ /10 <sup>-29</sup> e.s.u		
						B3LYP/6-31G(d)	CAM-B3LYP/6-31G(d)	BHHLYP/6-31G(d)
<b>Dye 1</b>	DMSO	5.56	1.90	6.55	6.20	6.29	6.15	5.10
	MeOH	5.53	1.59	6.52	4.98	6.21	6.07	5.04
	CHCl <sub>3</sub>	4.96	1.85	5.99	5.74	4.90	4.86	4.08
	Toluene	4.45	1.39	5.58	4.42	3.92	3.93	3.33
<b>Dye 2</b>	DMSO	11.11	1.66	6.11	5.68	4.91	4.90	4.05
	MeOH	11.06	1.59	6.08	5.34	4.84	4.84	4.00
	CHCl <sub>3</sub>	10.23	1.65	5.56	5.62	4.77	3.87	3.23
	Toluene	9.45	0.55	5.15	1.85	3.78	3.11	2.61
<b>Dye 3</b>	DMSO	4.50	1.32	8.16	5.72	2.09	5.25	3.15
	MeOH	4.47	1.56	8.12	5.18	2.02	5.15	3.09
	CHCl <sub>3</sub>	3.95	1.55	7.48	5.21	1.18	3.75	2.15
	Toluene	3.52	1.24	6.95	3.96	0.83	2.81	1.56
<b>Dye 4</b>	DMSO	6.37	2.26	8.60	8.38	9.44	10.51	7.85
	MeOH	6.34	2.06	8.55	7.06	9.29	10.36	7.75
	CHCl <sub>3</sub>	5.71	2.45	7.82	8.72	7.09	8.15	6.11
	Toluene	5.19	1.54	7.23	5.26	5.50	6.49	4.88
<b>Dye 5</b>	DMSO	15.08	4.29	10.11	26.08	43.95	47.36	39.77
	MeOH	14.93	4.81	10.10	26.12	43.16	46.41	39.02
	CHCl <sub>3</sub>	12.86	4.06	8.99	23.81	31.47	33.00	28.33
	Toluene	11.46	4.29	8.19	13.62	23.44	24.36	21.19

<sup>[a]</sup>Total static dipole moment by DFT (B3LYP/6-31G(d)); <sup>[b]</sup>Experimental first order polarizability; <sup>[c]</sup>Isotropic polarizability by DFT (B3LYP/6-31G(d)); <sup>[d]</sup>Experimental first order hyperpolarizability. <sup>[e]</sup>First order hyperpolarizability by using DFT

**Table 4.** TD-DFT vertical excitation and emission parameters of the styryl dyes **1-5** various solvents.

Solvent	TD-DFT absorption parameters				TD-DFT emission parameters			
	$\lambda_{\text{abs}}^{[a]}$ (nm)	$\lambda_{\text{abs}}^{[b]}$ (nm)	$f^{[c]}$	Major orbital contribution <sup>[d]</sup> (%)	$\lambda_{\text{em}}^{[e]}$ (nm)	$\lambda_{\text{em}}^{[f]}$ (nm)	$f^{[g]}$	Major orbital contribution <sup>[h]</sup> (%)
	<b>Dye 1</b>				<b>Dye 1</b>			
DMSO	447	411.2	0.5896	H→L (88.9)	499	453.2	0.553	L→H (93.4)
DMF	444	411.4	0.5929	H→L (89.1)	491	453.6	0.555	L→H (93.5)
MeCN	433	409.6	0.5678	H→L (87.8)	486	451.3	0.5364	L→H (92.9)
MeOH	436	409.2	0.5628	H→L (87.5)	494	450.9	0.5325	L→H (92.8)
EtOH	438	409.8	0.5724	H→L (88.1)	488	451.9	0.5387	L→H (93.0)
Acetone	433	409.4	0.5696	H→L (87.9)	494	451.9	0.537	L→H (93.0)
EtOAc	441	408.2	0.5692	H→L (88.4)	490	453.4	0.5164	L→H (92.4)
CHCl <sub>3</sub>	434	409.2	0.5883	H→L (89.6)	492	455.7	0.5164	L→H (92.3)
Toluene	432	408.5	0.5974	H→L (91.0)	488	452.3	0.7668	L→H (98.2)
	<b>Dye 2</b>				<b>Dye 2</b>			
DMSO	453	413.1	0.5117	H→L (80.5)	505	449.8	0.542	L→H (90.6)
DMF	450	413.3	0.5167	H→L (80.9)	494	450.1	0.5445	L→H (90.8)
MeCN	438	411.5	0.4842	H→L (78.2)	488	450.1	0.5445	L→H (89.9)
MeOH	438	411.1	0.4778	H→L (77.7)	497	447.7	0.5226	L→H (89.7)
EtOH	443	411.7	0.4914	H→L (78.9)	491	448.2	0.5255	L→H (89.9)
Acetone	439	411.5	0.4909	H→L (78.9)	494	448.2	0.5065	L→H (88.1)
EtOAc	439	410	0.5016	H→L (80.5)	498	445.3	0.6902	L→H (96.7)
CHCl <sub>3</sub>	443	410.8	0.5298	H→L (82.9)	497	442.5	0.7175	L→H (97.5)
Toluene	440	408.9	0.5539	H→L (85.4)	495	443.2	0.7364	L→H (99.2)
	<b>Dye 3</b>				<b>Dye 3</b>			
DMSO	453	452	0.9567	H→L (98.1)	533	529.9	0.857	L→H (99.4)
DMF	453	452.4	0.9593	H→L (98.1)	523	530.6	0.8591	L→H (99.4)
MeCN	445	449.8	0.9386	H→L (98.0)	518	526.9	0.8399	L→H (99.4)
MeOH	467	449.3	0.9344	H→L (98.0)	535	526.3	0.8358	L→H (99.4)
EtOH	469	450.3	0.9421	H→L (98.0)	539	528	0.8422	L→H (99.4)
Acetone	450	450.2	0.9409	H→L (98.0)	528	528.2	0.8405	L→H (99.4)
EtOAc	449	450.5	0.9363	H→L (98.0)	526	531.8	0.8301	L→H (99.5)
CHCl <sub>3</sub>	456	452.6	0.9503	H→L (98.2)	536	535.8	0.8419	L→H (99.5)
Toluene	452	453.8	0.95	H→L (98.2)	537	540.9	0.8388	L→H (99.6)
	<b>Dye 4</b>				<b>Dye 4</b>			
DMSO	478	460.4	0.9822	H→L (97.2)	551	529.7	0.8931	L→H (98.8)
DMF	466	460.7	0.9855	H→L (97.3)	535	530.4	0.8957	L→H (98.8)
MeCN	476	458	0.9628	H→L (97.0)	543	526.6	0.8756	L→H (98.8)
MeOH	465	457.4	0.9583	H→L (97.0)	543	526.1	0.8819	L→H (98.8)
EtOH	470	458.4	0.9671	H→L (97.1)	537	527.6	0.8789	L→H (98.8)
Acetone	466	458.2	0.9662	H→L (97.1)	542	527.6	0.8777	L→H (98.8)
EtOAc	463	457.2	0.9664	H→L (97.2)	545	530.1	0.8741	L→H (99.0)
CHCl <sub>3</sub>	465	459.1	0.9835	H→L (97.5)	543	533.8	0.8884	L→H (99.1)
Toluene	464	458.9	0.9878	H→L (97.7)	542	537.5	0.8903	L→H (99.2)
	<b>Dye 5</b>				<b>Dye 5</b>			
DMSO	535	537.5	1.1422	H→L (98.9)	670	587.4	1.0982	L→H (100.0)
DMF	528	538.1	1.1432	H→L (98.9)	664	589.2	1.0918	L→H (99.9)
MeCN	509	533.5	1.1196	H→L (98.7)	657	583.3	1.0691	L→H (99.9)
MeOH	501	532.5	1.1139	H→L (98.7)	659	582.4	1.0633	L→H (99.9)
EtOH	510	534.2	1.1188	H→L (98.7)	657	585	1.0679	L→H (99.9)
Acetone	507	533.9	1.1141	H→L (98.7)	639	585.1	1.0635	L→H (99.9)
EtOAc	515	532.9	1.0702	H→L (98.4)	650	588.9	1.022	L→H (99.8)
CHCl <sub>3</sub>	520	535.8	1.0766	H→L (98.5)	634	594.9	1.0211	L→H (99.8)
Toluene	507	534.9	1.0391	H→L (98.3)	619	600.3	0.9687	L→H (99.6)

<sup>[a]</sup>Experimental absorption wavelength; <sup>[b]</sup>Vertical excitations <sup>[c]</sup>TD-DFT oscillator strength of vertical absorption; <sup>[d]</sup>Major electronic transition for vertical excitation; <sup>[e]</sup>Experimental emission wavelength; <sup>[f]</sup>TD-DFT vertical emission wavelength; <sup>[g]</sup>TD-DFT oscillator strength of vertical emission; <sup>[h]</sup>Major electronic transition for vertical emission; (H=HOMO; L=LUMO)

---